National Aeronautics and Space Administration

Contract Order No. H-11992D
AP42-F/Michael Lalla
(205) 544-3948

Carl N. Lester EH-35
Marshall Space Flight Center, AL 35812

Final Report on the

SRB Frustrum "Smiley" Cracking Phenomenon Study

February 6, 1993

Revised February 26, 1993

Thomas A. Cruse, Ph.D.
401 Bowling Ave. #6
Nashville, TN 37205
(615) 343-8727; (615) 343-8730 (fax)

SRB Frustrum "Smiley" Cracking Phenomenon Study

1.0 Executive Summary

The purpose of the investigation is to determine the cause of cracking in the MSA-2 thermal protection system (TPS) used on the solid rocket booster (SRB) frustrums and to recommend changes that would eliminate the cause of the cracks. The MSA-2 material is a sprayed-on thermal protection ~~sealant~~ system composed of a curable resin with glass fibers, hollow phenolic and glass microballoons, and ground cork. The MSA-2 material is applied to the flight structure over painted metal or over a flexible system (PR-1422) covering exposed splice joints and mechanical fasteners. The MSA-2 material is then coated with hypalon paint which seals the system against any water intrusion.

Following post-flight recovery, the SRB nose frustrums are found to have various numbers of debonds of the MSA-2 material, with some number of these having cracks which extend through the hypalon paint. The debonds appear over and adjacent to the local regions of MSA-2 covered PR-1422 sealant. The cracks appear to extend between the metallic substrate and the free surface of the hypalon paint. Smaller cracks have the appearance of broken or split blisters, while the large cracks form portions of circular arcs, thereby giving them the name "smiley" cracks. All cracks are associated with debonds, and all debonds are associated with thickness transitions over the PR-1422 sealant. Finally, only a small percentage of the possible debond locations have, in fact, debonded.

The study has included a complete review of all documents presented by USBI to the consultant, a post-flight assessment investigation of "smiley" cracks performed by the consultant, a series of finite element method (FEM) analyses of various MSA-2/PR-1422 configurations, and a test program. Based on the FEM analyses, the consultant hypothesized that the source of cracking is a stress concentration formed by the presence of excess PR-1422 sealant which extends outward from the nominal seal area; the extension of the PR-1422 material, which is much more compliant than the MSA-2 material, creates a stress riser at or very near the interface between the MSA-2 and the PR-1422 material. Loading is provided by the depressurization of the external, hypalon surface just prior to SRB reentry from launch.

The quality of the bond between the MSA-2 and the PR-1422 materials also appears to play a role in the cracking problem. Physical evidence taken from the PFA of STS-50 by the consultant suggests that the bond line over the excess PR-1422 is weaker than at other locations. The suggestion of weakness arises because of the clean failure surface noted in these locations for samples taken which contain surface cracks. Adjacent regions of bonded MSA-2 and PR-1422 suggest much higher bond strengths in areas that did not debond in flight. The precise interaction between the appearance of clean surfaces (suggesting low strength) and the stress concentration at the interface causing debond has not yet been subjected to detailed examination. The combined role of the two issues above is taken to be the root cause of the cracking problem.

The fact that so few sites of those possible contain debonds and cracks suggests strongly that the problem is caused by the statistical combination of high stress concentrations at some of the PR-1422 sealant locations with excess material, and weakness of the bond strength at the material interface. The small number of critical locations also strongly suggests that the fix does not require major configuration or material changes. The problem is not an overwhelming problem. The recommended solution is to remove all excess PR-1422 material and to assure good interface strength by proper PR-1422 surface preparation.

d:\wp\consult\smile_f.rev

2.0 Past Studies and Reports

2.1 MSA Material Properties

The data cited in this section is summarized from the M&P report on MSA-2/PR-1422 bonding strength evaluation performed following the STS-48 divot anomaly [1]. Tensile strength is evaluated in two ways: flatwise tensile strength tests, and the *in situ* tensile strength test. The former generally produces higher strength than the latter, which may be due to better control over the loading of the material.

The cited report indicates that the ambient temperature flat tensile strength values for the MSA-2 material applied over bare sealant are on the order of 67-71 psi. In test results where the MSA-2 material was applied over painted sealant, the strength range was 10-14 psi. These tests are performed on flat test sections cut from prepared panels. The tensile strength of MSA-2 bonded directly to the substrate is reported in various locations to be 223 to 287 psi.

Preliminary thermal vacuum testing of panels with MSA-2 applied over the fastener bolt head area showed that 3 out of 5 locations with the lower strength did generate surface cracks (and, I must assume, associated debonds), while none of the higher strength configurations developed cracks. The implication of this testing is that depressurization can cause "smiley" cracks, if the debond strength of the interface is low. The report does not cite anomalous application of the low-profile caps, such as excess material which flows out from under the cap to form a second step in the PR-1422 profile. It is assumed that no such excess material was simulated in these tests, as the issue concerned the interface strength under bare and painted conditions.

Voids in the MSA-2 material play a key role in the failure scenario, as will be discussed in detail in the section on MSA-1 testing. The voids allow gaseous pressure, which is roughly in equilibrium with atmospheric pressure following hypalon material application, to load the MSA-2/PR-1422 materials under vacuum conditions prior to booster reentry. Porosity of the MSA-2 material is on the order of 20-40%, and equivalent to that of the MSA-1 system [2]. This same report cites that the strength of the MSA-2 material applied to a painted substrate is 150-180 psi, while that of the PR-1422 in the same configuration is about 203 psi.

2.2 MSA-1 Material Debond Testing

A key report on the nature of crack formation from MSA-2 debonds was generated for the MSA-1 material [3]. The findings of importance include the effect of elevated temperature on the strength of MSA material, and the role of implanted debonds of subsequent fracture strength of the MSA-2 material. When it was determined that depressurization could lead to the formation of "smiley" cracks over implanted debonds without any temperature effect, heating was dropped as a "smiley" test condition.

Nonetheless, USBI did contract for flatwise tensile testing of the MSA-1 material at test temperatures of 20°F, 74°F, 135°F, and 200°F. The testing was done of multiple samples and batches. The average strengths of the MSA-1 material for these test temperatures was found to be 274.8 psi, 243.8 psi, 154.62 psi, and 104.41 psi respectively. Thus, temperatures of 135°F and over have a pronounced effect on basic MSA-1 strength. The testing did not include PR-1422 interface strength testing.

Interesting data of some use in the report below is the tensile modulus data reported for MSA-1 material. The modulus data was taken from dynamic tests and is reported in terms of both the elastic and viscous terms of the response function. Ambient test conditions resulted in an elastic modulus value on the order of 15 ksi, while the value at 200°F is on the order of 7 ksi.

The summary chart of MSA-1 strength versus temperature taken from the cited report indicates that the hypalon paint undergoes a phase change at about 375°F. This value is important, as it sets an upper bound on the surface temperatures seen by the frustrums over their entire usage profile. Since no hypalon transformation is seen on the frustrums (but is seen on the aft skirts!), the outer surface temperature for the frustrums is less than (and probably significantly less than) 375°F.

The principal work reported in the cited document is the tests run on a panel containing multiple implanted debonds including circular debonds from 0.5" to 6.0", multiple debonds of 2.68", and a rectangular debond of 14" x 2.0". The debonds were implanted through the use of teflon coating of the substrate such that no bond took place. Testing was done in two ways: depressurization with temperature, and depressurization without temperature. Temperature was found to be unnecessary to the formation of "smiley" cracks and was dropped for convenience.

Loading experience included three approaches. In the first, the loading was applied as back face pressure which resulted in energetic liberation of the material covering the debonds. In the second case, depressurization of the panel was done, without sealing the edges of the panel. There was no indication of any "smiley" cracks for this test condition. The third test condition sealed the edges of the panels so that trapped gases in the MSA-1 material could not escape (hypalon being a vapor barrier material); during depressurization the debonds were seen to create "smiley" cracks.

The testing confirms that depressurization in the presence of debonding of the MSA-1 material can produce fracture of the MSA-1 material in a pattern that appears very similar to that seen on flight hardware. The mechanism is not unlike that of classical fracture mechanics. The pressurization creates a mechanical loading which is reacted only on the bonded interface. At the tip of the debond, the stress level in the bond line ahead of the debond can be quite high. When the stress in the MSA-1 material reaches some critical level in the material ahead of the debond, fracture of the MSA-1 material occurs and extends to the free surface, under or through the hypalon paint.

The data cited for these tests shows that the depressurization level can be correlated with the size of the debond to produce what has the appearance of an effective fracture strength parameter for MSA-1 material. Table I shows how that is done. The table cites the specimen configuration, the effective pressure acting on the debonded area, the effective debond size parameter (1/2 of the diameter or width, following the usual convention for cracks), and the product of the pressure load times the square root of the debond size parameter. It can be seen that there is a reasonable correlation of these values of "toughness" over the range of the testing.

Table I: "Fracture Strength" Model of MSA-1 Debond Tests

Test Condition	Pressure (psi) Δp	Debond size a(in)	$\Delta p \sqrt{a}$
Circular debond B1	6.2 psi	3.0"	10.74 psi $\sqrt{in}$
Circular debond C1	8.6 psi	1.3"	9.81 psi $\sqrt{in}$
Rectangular debond D1	9.9 psi	1.0"	9.90 psi $\sqrt{in}$
Circular debond B2	6.8 psi	3.0"	11.78 psi $\sqrt{in}$
Circular debond C2	6.7/8.8 psi	1.3"	8.84 psi$\sqrt{in}$
Rectangular debond D2	8.8 psi	1.0"	8.7 psi$\sqrt{in}$

If we assume that a full vacuum exists, the Δp value becomes 14.7 psi, and the effective damage size for the average "toughness," above, of 10 psi$\sqrt{in}$, then a "smiley" could form for a value of a=0.5" or 12.7 mm. The value of "a" will go down if we further take the effect of temperature rise into account, both in terms of strength and in terms of the pressure loading due to expansion of the entrapped vapors. The value above of 0.5" is within about a factor of 2 of the observed debonds with associated "smiley" type cracks. It is therefore concluded that the MSA-1 test results, together with the "smiley" failures cited in the section above clearly indicate that depressurization causes "smiley" cracks in the MSA-2 material above debonds. The MSA-1 testing does not indicate the cause of the debonds.

2.3 Flight Loading Conditions

Flight load conditions of some concern include depressurization, thermal growth of the TPS, temperature as it affects strength, and high mach number pressure acting to shear the material raised above the PR-1422 sealed fastener heads. Of these, only the depressurization loading and the temperature level affect on strength are taken to be significant loading variables. The reasons for including these two variables have been cited in the two previous sections.

The temperature levels on the raised bumps of MSA-2 over the fasteners will not be uniform, with respect to the flight direction. As discussed under the post flight inspection section, the tendency for debonds and "smiley" formation is on the upwind side of the fasteners, relative to the ascent flight direction. With few exceptions, the debonding and cracking favor this side of the raised MSA-2 material. Verbal communication with a NASA engineer analyst [4] indicates that the thermal loading of the frustrum is most severe during ascent, and that the upwind side of the raised material would have a somewhat higher temperature level, as compared to the downwind side. The conclusion is that the temperature level is playing some role in determining the failure locations. However, due to at least one downwind side "smiley" crack, the temperature role is not dominant. A transient heat conduction analysis of the MSA-

2/PR-1422 material configuration over a fastener has not been conducted; for sensitivity purposes, a temperature rise in the MSA-2 material of about 150°F has been used.

Temperature will affect thermal stress as well as strength. Using the values of thermal expansion supplied by USBI [2] of 5.5 x 10^{-5}(in/in/°F) for PR-1422 and 1.9 x 10^{-5} (in/in/°F) for the MSA-2 materials, and a temperature rise of 150°F, the maximum thermal stresses are no more than 3 psi. This effect is judged to be negligible.

Temperature rise will also increase the effective pressure of the entrapped gas vapors. Assuming the perfect gas law, we can compute that the effective internal pressure associated with a temperature rise of 150°F is on the order of 19 psi. This is a significant increase in the effective loading of the MSA-2 material.

Shear loading of the raised bumps was conducted by USBI. My review of that model has only been to confirm that the mechanical loads appear to be quite low. Further, these loads would only occur during the dynamic pressure loading part of the flight where the depressurization leading to "smiley" is not occurring.

2.4 STS-48 Observations

The STS-48 MSA Divot Anomaly Report [5] was reviewed prior to starting the current investigation, as well as numerous times since then. The observations and conclusions in the report are largely consistent with those I have made following STS-50. Some of the key findings in that report are as follows:

- A total of 328 debonds or "smileys" have occurred...with two exceptions, all occurrences were associated with fasteners. (p.2)
- The MSA-2 taken from the general acreage is very rough and broken. MSA-2 surfaces bonded to the PR-1422 covered fasteners are relatively smooth. (p.8)
- ...the initial debonding occurred near the MSA-2 to PR-1422 interface. (p.8)
- This data does not support the theory that debonds exhibit a banding effect ...(p.24)
- ...a visual review of the postflight maps does not indicate that more circumferential debonds occur inside than outside the debris zone. (p. 24)

The report did not reach conclusions regarding the formation of the debonds and the associated "smiley" cracks. The report did conclude that the formations occurred after the powered ascent phase of the flight. The report suggests that weakness of the bond at the MSA-2/PR-1422 interface played a role in the divot formation.

3.0 Post Flight Inspection Observations Made

The trip to KSC for the STS post flight inspection/assessment was made on 14 September 1992. The opportunity to observe the hardware provided a critical opportunity to build a picture of the common elements associated with debonds and "smiley" formation. The flight included, in fact, a divot of MSA-2 material involving a horizontal row of fasteners. Several representative and unique "smiley" crack formations were documented by removing the MSA-2 material surrounding the "smiley" crack and returning these to the MSFC. Photograph copies taken of the removed samples are included in an appendix to this report, along with rough notes taken during the PFA. The following paragraphs are taken from the trip report following the PFA.

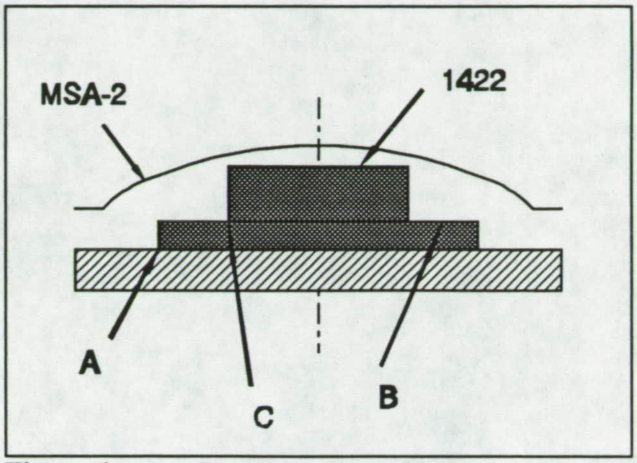

Figure 1: Representation of Material Configuration at Single Fastener

[*Start of trip report*]

I will begin with a summary of what I saw and what import I give to the observations. First, I think we need to generalize the definition of "smiley" cracks. There were numerous debonds of the MSA-2 over the fastener sealer. Many of these debonds had cracks of various sizes, orientations, and locations relative to the fasteners. According to those who report cracks, these are all "smileys" even though only some of them have the characteristic "smiley" shape and location. I observed a large number of these cracks and removed the MSA-2 material with crack at six locations. I have that material along with photos of the removed material and the frustrum site of the sample.

There was one divot on the frustrums, and I have the material from which the divot came. The debonds I observed were all over raised sealant material. Most debonds involved single fasteners, although there were some in the double row locations that involved two fasteners. One debond and "smiley" was located at an access panel, but again was over raised sealant. The USBI engineers fully documented the frustrum for "smiley" locations, and both video and still camera pictures were taken. My examination was sufficient for me to observe patterns and trends in the "smiley" types and locations, but did not constitute a full survey of the frustrums.

The negatives of the photos of the removed samples adjacent to their frustrum site are enclosed with this report in the hope that you can get blow-ups of the central part of the photos showing the site and the removed sample. The prints I have are useful only for cataloguing the material, not for documenting the surface from which the material was removed.

I also examined the condition of the MSA on the aft skirt. There were at least two divots on the aft skirt; one was associated with a sealed fastener and one covered an access panel of sorts with flush fasteners. The divots were larger than that found on the frustrum. There was some evidence of white "sooting" on the edges of and within the divot, indicating to Bob Henry that the divot was formed prior to or during separation.

Examination Details and Preliminary Findings:

The figure indicates the essential features of the material arrangement in the area of a single fastener. Examination of all of the removed specimens containing various sizes, shapes, and orientations of cracks including the specimen with the divot indicated that each appeared to have common elements which are seen to be critical to understanding the "smiley" problem. Locations A, B. and C are all locations of an appearance of weak bonding between the MSA and substrate materials. Locations B and C have 1422 sealant as the substrate, while location A has base metal as the substrate material. Location C is the site of the undercut associated with the caps that are used for sealant application. The sealant between sites A and C is the overfill sealant from the application procedure and has variable thickness. In one case, the 1422 sealant was seen to extend beyond site A on the metal substrate but with very little apparent thickness. It would seem that the cleanup of the overfill resulted in a regularly-sized "smear" of 1422.

I have enclosed, for the records, xerox copies of my raw inspection notes of those debonds and "smileys" that I focused on. I have noted what I believe to be the sites from which the samples are taken. I did not choose to document specific locations for the samples as I consider them to be representative of a phenomena that did not appear to have particular site-specific features.[1]

With only one major exception, all of the debond/cracking appeared to be on the up-wind side of the fastener (in the case of single-fastener row locations and some double-fastener row locations) or on the side of the double-fastener rows, or to cover the entire fastener. The exceptions included a noted site where the debond occurred on the downwind side of the fastener. That site is among those I selected for material removal. These are sites that can be expected to have higher heat flux during the ascent part of the flight. Based on USBI data subsequent to the PFA inspection, the frustrum sees its highest heat-loads during ascent, whereas the aft skirt sees its highest heat loads during reentry. All cracks are associated with debonds.

In all cases, the flexibility of the debond seemed to be quite similar in the sense of the resistance of the debond to local finger pressure. Of course, large debonds were more flexible, overall, than the smaller debonds, but in no case did it seem that the debond involved only the hypalon or hypalon and a small amount of MSA-2. Of course, this is a subjective opinion.

In all cases where I removed material containing a debond with a crack, the debond affected a larger region than the size of the crack - the physical appearance supports the hypothesis that the crack comes after the debond. I saw no exceptions to change this hypothesis. Further, and much more critically, the removed material at the debonds indicated quite clearly

---

[1] **These figures are in the original full Trip Report filed with Mr. Carl N. Lester, EH-35**

very low strength of the bond at site B in the figure, corresponding to the MSA-2 bond on the overfill bead of the 1422 sealant. The very low strength conclusion is based on the lack of adhesion of the MSA-2 to the 1422 indicated by MSA-2 "fuzz" which is clearly seen on other locations of the debond. Examination of the witness surface on the MSA-2 material I removed showed a consistent picture - the MSA-2 surface at location B was quite smooth and had the appearance of a mold of the 1422 sealant.

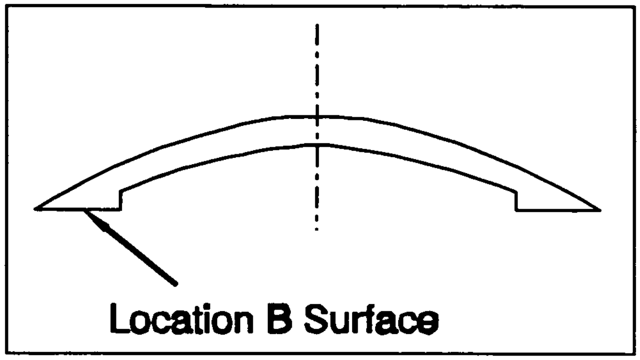

Figure 2 Cap Configuration Used for Sealant Application

Examination of the six debonded regions also shows that the adherence of MSA-2 to the supporting material is weak at locations A and C. In no case did the weak bond of MSA-2 to base metal extend more than a few mils from the edge of the 1422, but the metal surface clearly showed a lack of retained MSA-2 over a significant arc length of the failed zone. The radial extent of the weak bond is consistent with the size of the "voids" noted in the report on STS-48 that I read. The MSA-2 fractures were all featured as conical failure surfaces at roughly 45° to the substrate. The small radial extent of the weak bonded surface indicated to me that this location was not primary, but secondary in the sequence of MSA-2 fracture.

The weak bond of MSA-2 and 1422 sealant is radially large compared to that at location A. The weakness may include both locations B and C. The undercut showed very little likelihood of good bonding between the two materials. However, the size of the weak region associated with the overfill surface (location B) appears to be large enough to allow fracture associated with the depressurization event near the point of separation, when the external pressure at the hypalon is at its lowest point. Such depressurization fractures of the MSA-2 material were shown in the USBI M&P test report, without the need for external heating. In removing the MSA-2 material from the selected sites, I qualitatively noted that the bond to the crown of the 1422 sealant in cases where the debond did not include this region, was quite strong in comparison to that strength I noted in peeling the material from location B.

The question remains as to why the debond occurs, and why does it occur at the observed sites with the observed frequency. The dominant feature of the debonds occurring on the up-wind or side locations (in the case of double-fastener rows) is strongly suggestive that the heating causes mechanical loads of the MSA-2 material due to both thermal expansion, depressurization, and entrapped gas expansion. The local curvature of the MSA-2 over the 1422-sealed fasteners under such loading will create tensile stress on the bonded interfaces. The details of this stress condition are subject to the local details of the material geometry, which is highly variable. The planned FEM analysis of a representative configuration will confirm the essential features of the debond stress distribution.

The observations are strongly suggestive to me that, while all MSA-2 sites which cover raised regions of fastener/panel/sealant are subject to the stresses just described, a statistical range of bond strengths between the MSA-2 and the 1422 sealant at location B permits the number of observed debonds. The critical fact is that the vast majority of the bonds are strong enough to resist this loading. This clearly means that the stress levels are not extremely high, relative to the nominal strength of the bond. It does suggest, though, that one of the two following issues are critical: (1) their exists a likelihood that some of the overfill surfaces are in some way contaminated such that un-typically weak bonding occurs; or (2) that a relatively minor stress reduction on the bond line will eliminate the debond problem. If there are no debonds, then there will be no cracks.

At this time, there is no clear preference for one theory over the other, of the two cited above. The FEM analysis can shed some light on the issue, but its strict applicability in a quantitative sense is going to be limited by our confidence in the material properties used, especially the thermal swelling of the MSA-2 due to entrapped gases. The requested thermal expansion test of a coated aluminum panel should be conducted with the edges of the MSA-2 sealed, as was done in the USBI M&P testing of MSA-1, a few years ago. Strength testing of a panel with 1422 sealant applied in the usual way would require too many fasteners to be very practical; the large number of fasteners would be required to develop a meaningful statistical minimum strength over the raised features.[2]

The fact is that the sealant is applied by hand. The amount of sealant applied is quite variable (I was given the opportunity to observe the USBI sealant operation at Hanger AF). By this letter, I am requesting a review of the methods used to assure that the green caps used to apply the sealant are not contaminated on the external base (see the adjacent figure), and that the sealant surface roughness or other physical characteristics between the crown location and the flat associated with location B are qualitatively the same.

[*end of trip report*]

Following the PFA, the determination was made to perform finite element method (FEM) analysis of the MSA-2/PR-1422 configuration, with special emphasis given to the role, if any, of the excess material that occurs under the low-profile cap, in many cases of PR-1422 sealant application. All of the above observations indicated that the debonds were focused over the region of excess material and that the interface bonding in the region of the debond seemed less effective than for interface bonding at other locations.

Subsequent to the PFA, the issue of interface bond strength was reviewed to determine if the thickness of the MSA-2 material in this region could reduce the interface strength. While the data is suggestive that the strength does, in fact, reduce, with thickness of the MSA-2 material, the decrease, as tested, does not seem to support being the sole cause of the debonds.

---

[2] The FEM analysis resulted in a changed test strategy in that thermal expansion was found to be an insignificant source of stress. Overfill of PR-1422 sealant was found to be the probable source of the local failures [Note added on February 26, 1993].

The PFA brought out very much the statistical aspect of the problem. By far, most fastener locations did not have debonds. Most debonds did not have "smiley" cracks. Thus, we are faced with trying to find, by analysis and test, a failure mechanism that involves only the tail of the failure distribution, where higher than normal stresses and/or lower than usual strengths are involved. The risk exists that no experimental method can fully document this "tail" problem.

4.0 Finite Element Analyses

4.1 Assumptions and material values used

The FEM modeling assumed that both the MSA-2 and PR-1422 materials were elastic and homogenous materials which were perfectly bonded together. The aluminum substrate was taken to be infinitely rigid (a much higher modulus than either of the non-metallic materials). Loading was taken to be an externally applied tensile pressure of 14.7 psi. The loading corresponds to the condition of the loss of atmospheric pressure acting internally and externally on the system prior to launch. Thus, the simulated stress is taken as the sum of that obtained by the FEM model and -14.7 psi, corresponding to the ambient stress condition. The effective stress measure of strength is used, as the material sees multiaxial stresses under the FEM loading conditions; the effective stress measure under ambient loading conditions is zero.

Initial FEM runs were made with a modeled temperature rise of 150°F on the MSA-2 material, with no temperature rise in the PR-1422 or substrate materials. This was taken to be a very simple way to confirm that the thermal stresses were negligible. The thermal component of the stresses was indeed negligible and the elevated temperature thermal stress issue was therefore dropped.

The effective stresses were computed at the vacuum conditions of the applied normal stress of 14.7 psi, as stated above. No account was taken of the probability that the elevated temperature, in fact, would raise the internal pressure within the MSA-2 material. However, the degree of vacuum actually encountered was not considered, and it has been assumed that 14.7 psi is a conservative level of the applied stress to use.

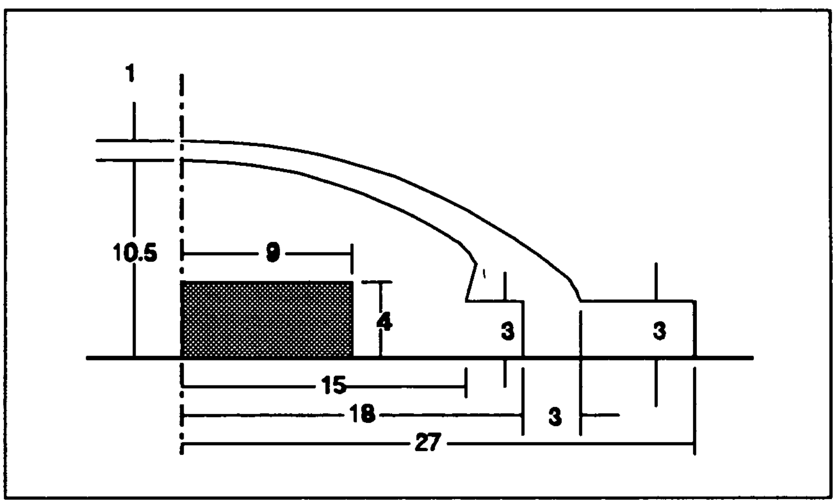

Figure 3: Nominal Dimensions of FEM Model (mm.)

The modulus of the PR-1422 material was reported [2] to be approximately 100 psi. The value for the MSA-2 material was cited to be at least an order of magnitude higher. For the sake of conservatism, the value of 1,000 psi was taken. This will be further discussed in the results below. The value of Poisson's ratio was taken to be 0.2, using a rule of mixtures between the matrix value taken (0.35) and that for the void content, taken to be 30%. Lower values of Poisson's ratio will tend to reduce the localized stresses that are calculated.

The nominal geometry defined for analysis is shown in Figure 3, where the dimensions are given in millimeters. The configuration is taken to be axisymmetric, and only the right-hand side of the geometry is shown. The nominal geometry has been taken to have a large amount of excess PR-1422 material, taken to be 3 mm thick and extending to the edge of the low profile cap, which has been removed. The right hand edge of the indicated geometry is taken to be a surface with no normal motion of the MSA-2 material, thereby approximating the restraint of the surrounding MSA-2 material. The slight undercut of the low profile cap has been simplified by using an angle to the interface. The volume occupied by the fastener is indicated by the shaded region. The MSA-2 material is shown with a 1 mm thickness at the centerline, and a 3 mm thickness away from the fastener.

4.2 Finite Element Analysis Models and Results

The approach taken for the FEM modeling was to perturb the solutions relative to the above baseline case, in order to determine the sensitivity of the stresses to various of the critical geometry and material variables. The solutions were generated using the ANSYS® finite element program, version 4.4A, as developed and released by Swanson Analysis Systems, Incorporated. The axisymmetric, elastic stress analysis element, type 82, was used for the analysis. Loading was taken as applied pressure loading of -14.7 psi, applied to the top surfaces of the MSA-2 material. The hypalon was not included in the FEM model, just the effect of its presence in producing the depressurization loading.

The effective stress response variable is the one cited for reporting the results. This variable is selected because it combines all of the active stress components in a single, scalar variable, it has a zero value under nominal ambient pressure equilibrium, and because it may reflect the failure criteria reasonable well. The short-coming of the effective stress measure is its lack of any hydrostatic stress. Given that MSA-2 is porous, we cannot rule out a role of the hydrostatic stress in the failure of the material. However, lacking any multiaxial failure criteria for MSA-2 material or the MSA-2/PR-1422 interface, we will follow rather common practice in using the effective stress measure.

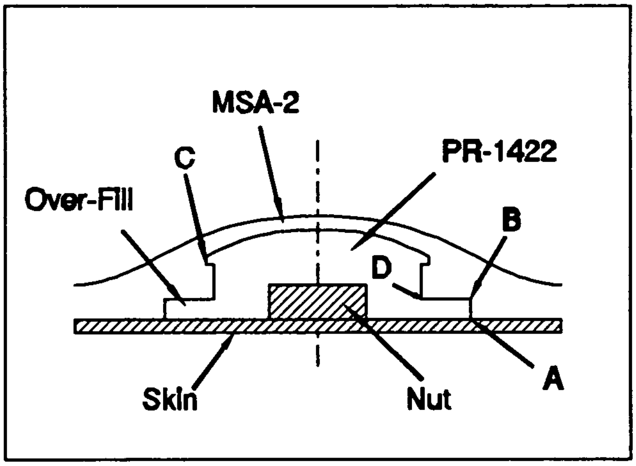

Figure 4: Schematic Showing Key Locations

The variations selected for the study include the thickness of the excess material, taking 0 mm (Case 3) and 1.5 mm (Case 5) as the other thickness. The shape of the low profile cap was changed to make an acute angle to the substrate, as opposed to a right angle intersection (Case 6). The amount of thickness of the MSA-2 material over the region of excess PR-1422 was reduced for one run (Case Y). Finally, the modulus of the MSA-2 material was doubled to 2,000 psi for one analysis (Case X). Some additional runs were made to simulate debonds on various surfaces. These runs will only be briefly mentioned below.

The results of the stress analyses for all cases involving excess PR-1422 material show that the maximum effective stress occurs at location B, as indicated in Figure 4. The mechanical cause of the high stress at this location is the re-entrant corner formed by the MSA-2, and the fact that the MSA-2 material is much stiffer than the PR-1422 material. The load being carried by the MSA-2 material over the PR-1422 sealant must turn the corner at location B, and then flow to the substrate at location A. The high stress region focused at point B extends into the MSA-2 material, somewhat along the interface towards location A. Stress contour results for the various cases are given in the appendices to this report. The maximum stresses are not to be taken too literally, as they will increase as the size of the finite elements near location D is refined. All FEM model results are based on the same mesh refinement near the stress concentrations, in order to make the comparisons, at least, meaningful. The following table summarized the results for the FEM solutions involving geometries with excess PR-1422 material, shown above as the overfill region.

Table II: Effective Stress Results for Selected FEM Models

Stress Case	**Max Effective Stress (psi)**	**Ratio to Baseline**
Baseline: Case 2	47 psi	1.0
No overfill: Case Z	31 psi	0.7
Reduced overfill thickness: Case 5	47 psi	1.0
Increased modulus: Case X	85 psi	1.8
Reduced MSA-2 thickness: Case Y	56 psi	1.2

4.3 Finite Element Analysis Conclusions

The results are normalized to the Case 2 maximum effective stress computed by the fixed FEM grid. Equivalent element sizes gives us some degree of comparability. However, the volume of material that sees the stress concentration is a factor influencing strength. There is no analytical model for a size effect in the material interface under consideration. Thus, the comparison in Table II should be taken as qualitative in nature. In all cases, the maximum stress is at an interface location. Contour plots of the effective stress are shown in the Appendix but are hard to read owing to the low quality graphical output capability available for this study.

Case Z was for no excess material. When the excess material is removed, the maximum stresses occur at location D which is now located at the interface with the skin. The stress concentration at this location is about 70% of that for the configuration with overfill. Case 5 considered a significant reduction in the thickness of the overfill; no significant change in stress was detectable. The conclusion is that, so long as there is more thickness in the overfill than a thin film or skim, the apparent stress concentration factor increase will occur. The actual stresses computed by the FEM analysis are very sensitive to the material modulus, as shown in Case X. Thus, only the ratios should be taken as real values. Finally, Case Y considered the effect of reducing the assumed thickness of the MSA-2 material covering the critical region. Thinner MSA-2 leads to higher stresses, as the interaction with the loading is closer to the maximum stress location for thinner MSA-2 material. A reduction in thickness by about a factor of 2 increased the local stress by about 20%. This influence is not taken to be critical at this time as none of the failure locations gave evidence of local underfill of the MSA-2 material.

The FEM analysis therefore strongly suggests that the excess material should act to reduce the strength of the MSA-2/PR-1422 bond, Further, failure should occur from locations near the corner of the excess PR-1422 material (location B). The strength reduction due to the stress concentration is of the order of 30%, based on these results.

5.0 Recommended Test Plan

A recommended test program was devised for the purpose of testing the above FEM results. The testing made use of standard test methods to the extent possible. The material presented in this section corresponds to the test plan submitted by the Consultant to NASA.

5.1 Test Overview:

Testing was to be performed on two sets of twenty test specimens; one set to be MSA-2 material tested at room temperature, and one at 200°F. Each of the two sets of test specimens was to be taken from two simulated sealed fastener conditions cut from coated aluminum panels. One condition at the simulated fastener locations was to contain significant, yet typical PR-1422 material overfill, while the other set was to have no overfill. Each panel was to be covered by MSA material using normal spray procedures.

Square (2" x 2") test specimens containing the simulated fastener were cut from each test panel. Pull blocks simulating external depressurization were bonded to the raised surface over each simulated fastener and are then pulled to failure. The failure loads are compared as an average for each set of locations. The ratio of the average overfill failure load to the average no-overfill failure load is calculated; the ratio is to be defined as the overfill strength reduction factor.

Standard testing of the strength of the MSA-2 material was performed on witness panels; one set of tests at ambient temperature, and one at the elevated temperature of 200°F.

5.2 Panel Preparation:

The test panels should be prepared in a fashion similar to that shown scematically in Figure 5. Each test panel of 0.125" thick aluminum contains four rows of five simulated fastener locations. The figure indicates typical locations for each of the 20 simulated fasteners, which are arranged in alternate rows of five with overfill, five without, etc. The simulated fastener locations were located on centers approximately 10x the size of the raised region which includes the PR-1422 material, and the raised MSA-2 material covering the sealant. The distance is to provide space sufficient to isolate each test location from all others, and for cutting each test specimen such that the 2"x 2" test specimen is large enough to minimize the influence of edge failures during tensile testing.

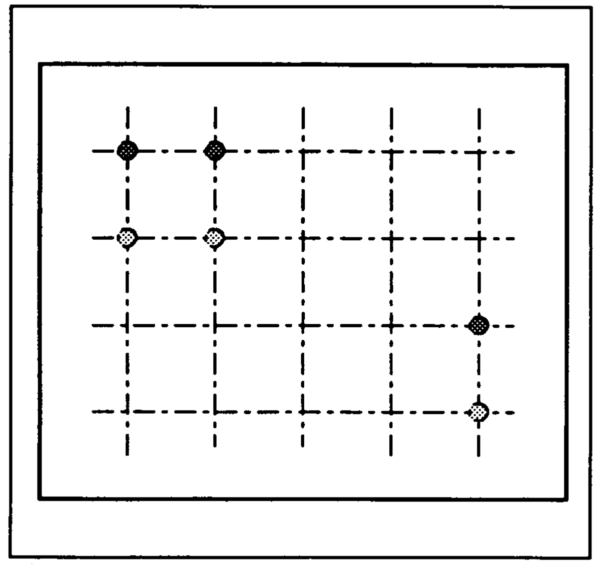

Figure 5: Proposed Test Panel

Trial-and-error methods are needed to determine the amount of PR-1422 sealant to add to each of the standard green sealant cups used over the fastener locations. Excess sealant will require substantial overfill of the green cup in order to achieve a relatively thick overfill extension. The thickness required is best judged from the examination of the specimens returned from the post-flight assessment review trip; current estimates are that the thickness to be on the order of 3 mm.

Specimen locations with no excess material will require that the green cup be slightly overfilled in order to assure 100% contact. It is possible that a hand rotation of the cup after pressure is applied holding the cup to the metal substrate may by sufficient to squeeze out all excess material other than a thin film of PR-1422. After the PR-1422 has cured, a plastic chisel may be used to remove the excess PR-1422 material from around the normal "cap" of PR-1422.

Twenty square tensile test pieces were cut from each test panel with simulated fasteners. The test pieces are each to be 2"x 2", following normal procedures for cutting test specimens from aluminum test panels. Each test specimen was to be labeled in a manner that defines the test specimen panel and panel location, relative to a reference location on the panel. The objective was to preserve a record that determines the location of the test piece relative to the variables involved in the spray and curing history of the panel.

5.3 Tensile Strength Testing:

Test pull blocks were fabricated for each of the 20 simulated fastener specimens cut from each test panel. Each block was of sufficient size that it could be bonded over the raised MSA-2 material for a bonded diameter approximately equal to the anticipated failure zone, as shown schematically in Figure 5.

To the extent possible, the locations with overfill (shown) and those without overfill were bonded to the pull block over the same diameter. [Note: Due to time constraints and a limited number of specially fabricated pull blocks, only five specimens of each configuration (with and without overfill) were tested at each temperature.]

5.4 Failure Sequence:

It was anticipated that failure of the locations with overfill will initiate at location B. Disbond will extend from B to locations A and C and beyond C toward the centerline, along the material interface. It was not known how suddenly the disbond along this path will be. At this time, I assume that the bond will remain intact up to some critical load level at which the disbond occurs. Following disbond, the load deflection curve is likely to be more compliant, indicating that there is softer support for resisting the pull bar. The break point is indicated in Figure 6 as point B. Final failure will likely occur as a separation along the path indicated as the estimated failure site.

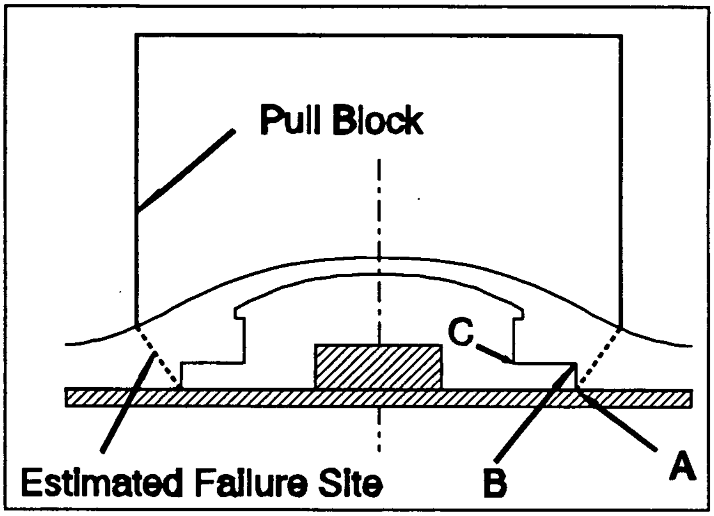

Figure 6: Schematic of Local Failure Region and Test Block

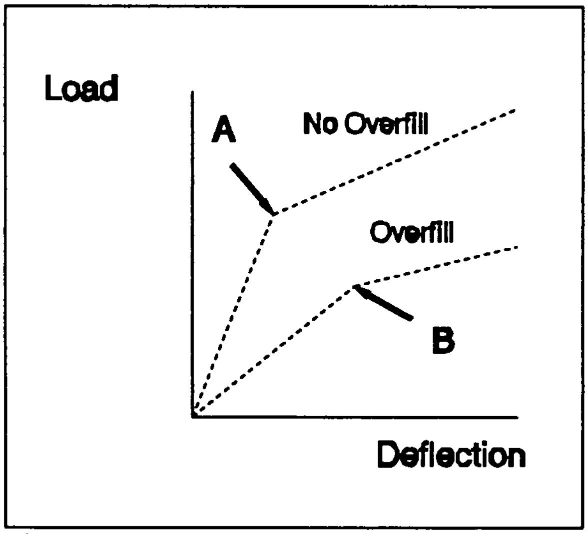

Figure 7: Schematic of the Load-Deflection History for the Pull Test

The pull test for no overfill of the PR-1422 material will show less compliance than for the test with overfill. The reason is that there is more MSA-2 material between the pull bar and the aluminum panel, to resist the applied loading. At a critical load level, the MSA-2/aluminum bond will fail (indicated in Figure 3 as point A). The loading will shift more toward the MSA-2/PR-1422 interface centered over the simulated fastener location. This load path is much more flexible than the original load path prior to bond failure and the load deflection curve will likely show a significant increase in compliance. Failure at the indicated failure site in Figure 6 will likely occur at point A in the load history.

During the individual pull tests, it is important to perform visual examination of the material around the pull test in order to document any indications of surface failures at the appropriate load levels. The load deflection histories should be recorded for later interpretation. Any failure indications are to be recorded according to the load level at which the indication occurred.

The estimated initial failure load for specimens with overfill is approximately equal to 15 psi times the bonded area projected onto the test panel. The ultimate load for all tests is on the order of 75-100 psi times the projected area of the bond, consistent with normal material strength.

5.5 Data Reporting:

Photographic recording of the test was supplemented by VCR recording. The load-deflection history for each pull test was recorded. Recording and observation is to be done consistent with the above estimates of initial and ultimate failure load levels.

The post-failure state of the material was preserved and photographed. The nature of the bond between the PR-1422 and the MSA-2 materials is especially important to document for the overfill case. The quality of the bond of the MSA-2 and the aluminum should also be verified by visual inspection of the failure surfaces. The size of the sealed material over the simulated fastener is to be recorded. The diameter of the failed region is to be recorded. The ultimate loads plus any loads indicating intermediate break-points in the load-deflection histories should be recorded. Any visual indications of failure should be recorded along with the load level associated with the visual report.

5.6 Assessment of the Experimental Results

The testing was largely successful. The test pieces were successfully fabricated and failure surface appearance seemed consistent with the PFA in that interface fracture took place on all test pieces. In many cases the painted aluminum surface is seen near Location A in Figure 6. The interface at the PR-1422 curved surface above the nut location failed on all tests, as expected; good bonding of this surface was observed.

The load-deflection curves did not show the anticipated break points associated with initial failure of the interface at Location B. The reason is most likely that the original hypothesis of a failure of the bond with enough residual strength in the MSA-2 material from Location A to the free surface is not correct. Apparently, the debond occurs at sufficiently high a strength that the remaining ligament of MSA-2 material cannot support the load without fracture. The load deflection curves do show some evidence of a tearing failure, though, rather than an abrupt fracture from the metal interface (Location A) to the free surface.

There is also some evidence from the appearance of the surfaces that the bond to the excess PR-1422 material is as strong as that over the cap itself. The appearance of MSA-2 material on the PR-1422 in the region of the overfill suggests that the test panel strength of the bond is greater than that of at least some of the failures noted in the PFA investigation of STS-50 "smiley" cracks. A strong bond here will also reduce the tendency for a breakpoint in the load deflection curve.

The test data for the four test conditions were averaged for comparison. The results are given in Table III. The data averages, standard deviations, and coefficient of variations (COV) are computed for each of the four test conditions. The effect of temperature on strength reduction is given by dividing the average elevated temperature strength by the corresponding value for the 200°F condition. We see that the elevated temperature results in about a 70% strength reduction, consistent with earlier test data. The effective stress concentration for the test data is computed by taking the average strength with overfill and dividing by the no-overfill strength. The data suggests that the strength reduction is between 18% (RT) and 29% (200°F). These values are in good agreement with the FEM prediction of about 30%.

Table III: Test Results Summary

Overfill RT		Overfill 200 F		No Overfill RT		No Overfill 200 F	
Specimen	Load_f	Specimen	Load_f	Specimen	Load_f	Specimen	Load_f
4-6	236	4-11	59	1-6	183	2-1	52
4-7	177	4-12	20	1-7	155	2-2	87
4-8	219	4-13	67	1-8	258	2-3	100
4-9	177	4-14	71	1-9	273	2-4	52
4-10	139	4-15	68	1-10	253	2-5	76
Average	189.6		57		224.4		73.4
Std Dev	38.4		21.2		52.1		21.3
COV	0.20		0.37		0.23		0.29
Temp Reduct			0.30				0.33
Effective K_t					1.18		1.29

The question of validity of the data must also be considered. Given that we have five samples for each test condition we must consider the importance of scatter. The elevated temperature test data shows a significantly higher scatter than the room temperature test data, especially the case with overfill. Given the variability in the geometry of the overfill and its closeness to the edge of the 2"x 2" test blocks, the higher scatter seems not too surprising. Specimen 4-12 does show some evidence of an edge failure in that the aluminum surface is exposed only near the edge, not near the PR-1422 material which is the case in the other specimens.

6.0 Conclusions and Recommendations

If we leave all of the data in the comparisons, the differences between the average strength values with and without overfill are approximately one standard deviation separated. The separation is therefore taken to be sufficiently great to conclude, at least informally, that the effect of the overfill in reducing the strengths is real. By application of the student-t test to the data we can conclude with at least 75% (but less than 90%) confidence that there is a positive difference between the means of the two sets of samples. When the data are pooled by scaling the means to the temperature effects, the variance increases too much for the means to be distinguished with even 75% confidence. By throwing out one low point in each pooled sample, we are once again able to distinguish the means with a bit more than 75% confidence.

Thus, even given the small sample and the scatter which may be associated with the test method as well as the material strength itself, I conclude that a reasonable likelihood of a significant strength difference between the overfill and no-overfill cases has been demonstrated. The likely level of the difference between the two strength levels is of the order of magnitude predicted from the FEM analysis.

However, it is also concluded that the strength of the test pieces may overstate the actual strengths in the flight vehicle case. This conclusion is drawn based on discussions with the technical monitor for the project, Mr. Carl Lester, who indicates that the excess material was roughened for the test program and that it may not always be sufficiently roughened in the flight hardware. Visual differences between the failed test pieces and the flight hardware inspected from STS-50 suggest that the unroughened surface does not have the interface bond strength of the roughened surfaces. Thus, even greater strength differences can be expected between the installed PR-1422 sealant with no excess material and that with excess material.

It is therefore recommended that installation of the PR-1422 sealant be accomplished without any excess material beyond the volume contained within the plastic cap. Further, FEM analysis suggests that a cap internal configuration which makes no angle to the aluminum surface will have less local stress concentration than the current configuration. The different stresses are contained to a small volume though, and the magnitude of the strength increase may not justify the expense of a new cap geometry.

Voids are sometimes seen in the region adjacent to the PR-1422 edge and since this is a region of elevated stresses, steps should be taken to spray the MSA-2 material in such a way as to minimize the occurrence of these voids. Evidence of the void problem may be the presence of white painted aluminum surfaces under debonds without strong evidence of good bonding of the MSA-2 material.

Thus, the original hypothesis that process quality issues are involved in the "smiley" cracking problem seems to be born out. Elimination of the occasional excess material totally is seen to be a likely way to eliminate the small percentage of PR-1422 sealant locations which debond. The use of hand operations to apply the PR-1422 material is seen as undesirable. A higher modulus replacement to the PR-1422 sealant will also reduce the discontinuity stresses along the MSA-2 interface, as found by the FEM analyses.

References

1. S. V. Patel, Internal Correspondence Memo to W. A. Riehl, "MSA-2/PR-1422 Bonding Data from Development Studies," M&P-4041-147-91, 23 September 1991.

2. A. K. Patel, USBI Senior Materials Engineer, communicated in response to letter from T. A. Cruse to C. N. Lester, 29 August 1992.

3. W. A. Riehl, R. Richardson, R. Thompson, D. Comer, G. Cooch, "MSA-1 Failure Analysis," unnumbered M&P branch report, USBI, March 1989.

4. Lee Foster, ED3, private communication.

5. W. A. Riehl, D. Comre, R. Raley, and R. Richardson, "STS-48 Divot Anomaly Investigation Team Report," USBI Report 2134-100, undated.

Appendices

A. Photographs from post-flight inspection

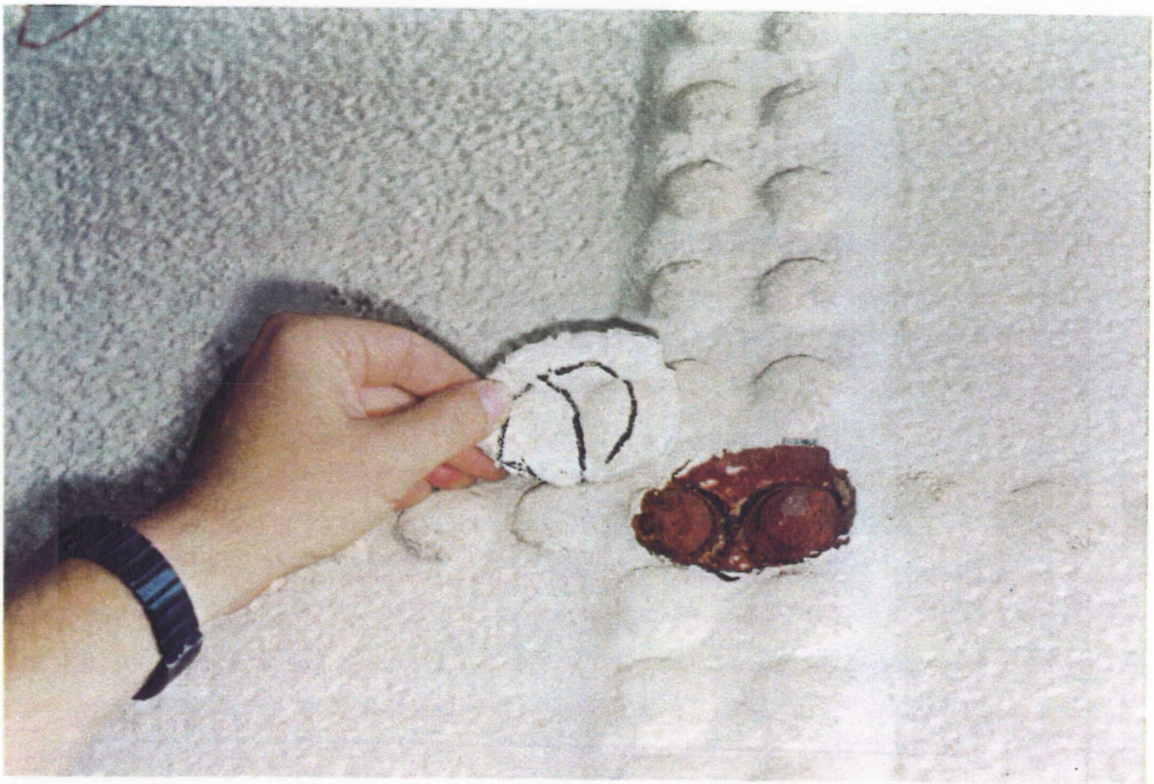

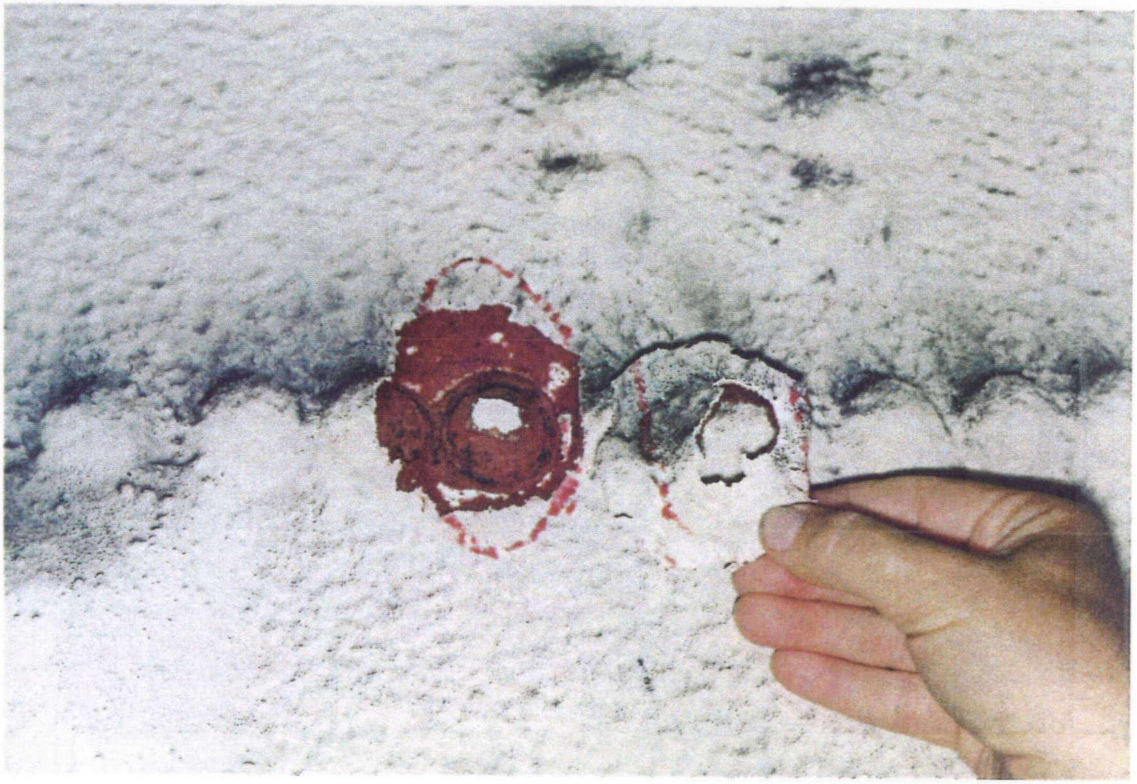

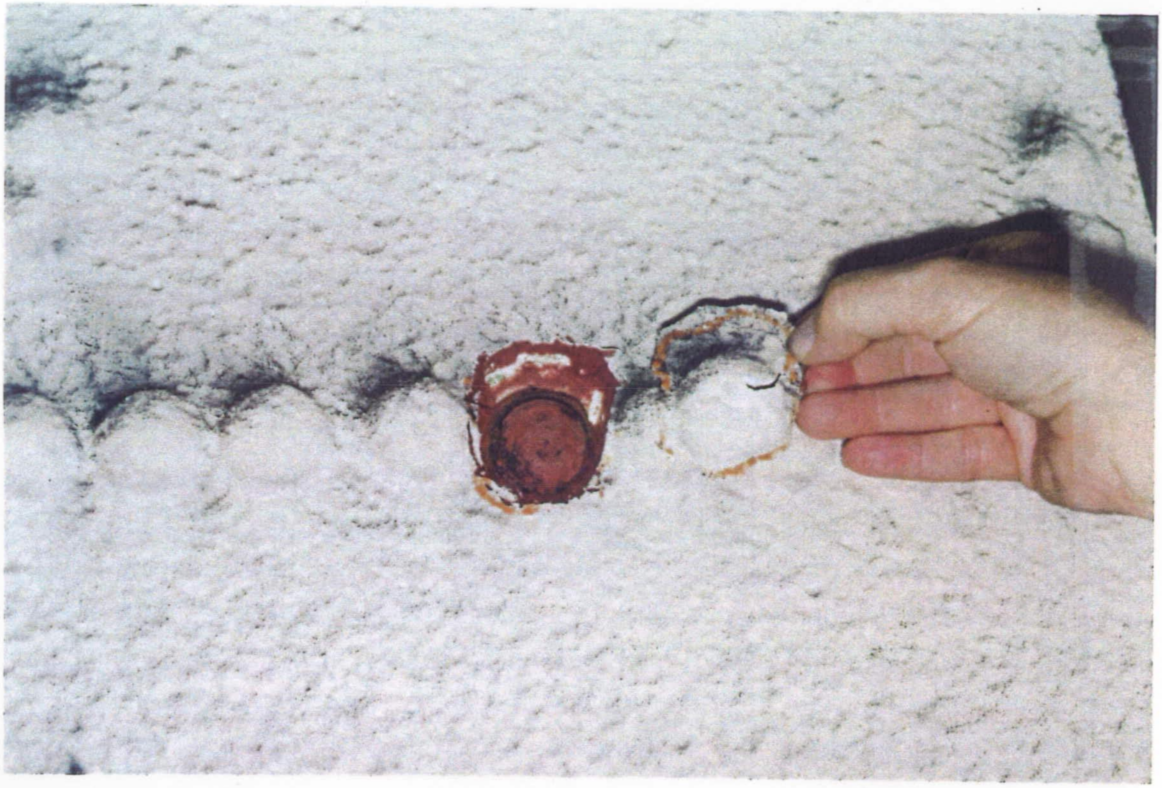

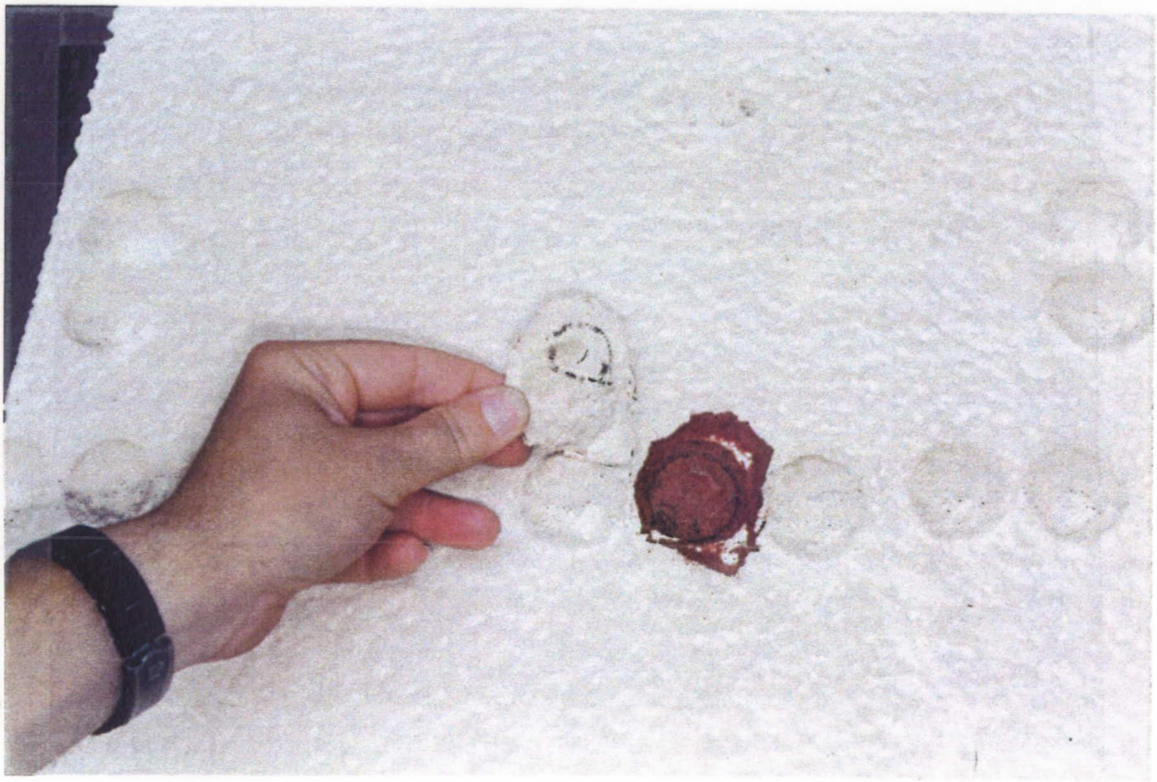

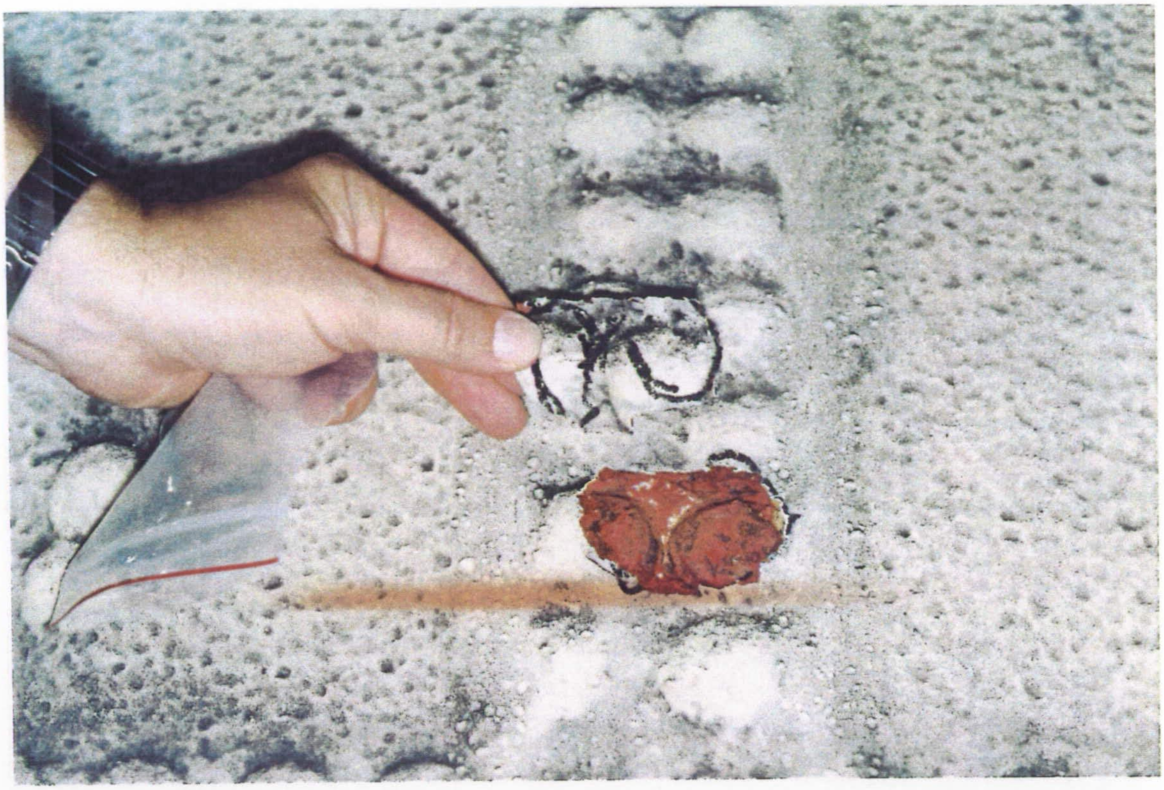

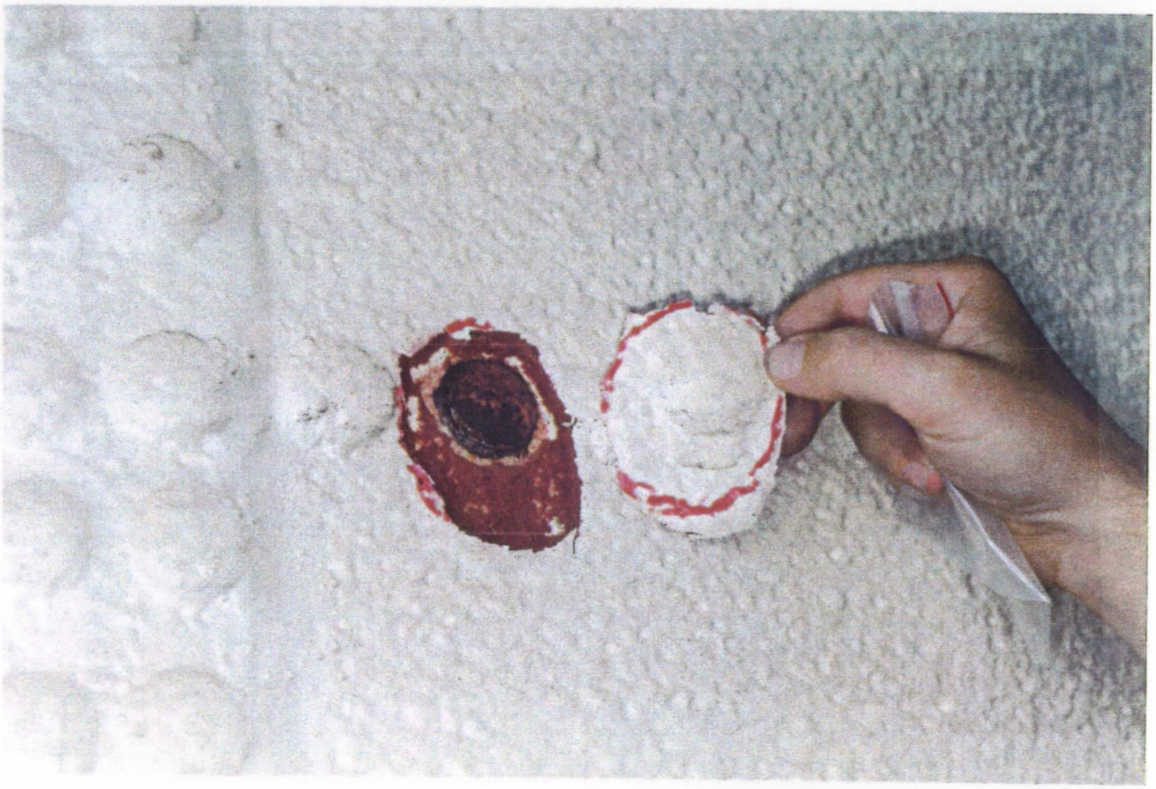

B. Finite Element Stress Contours

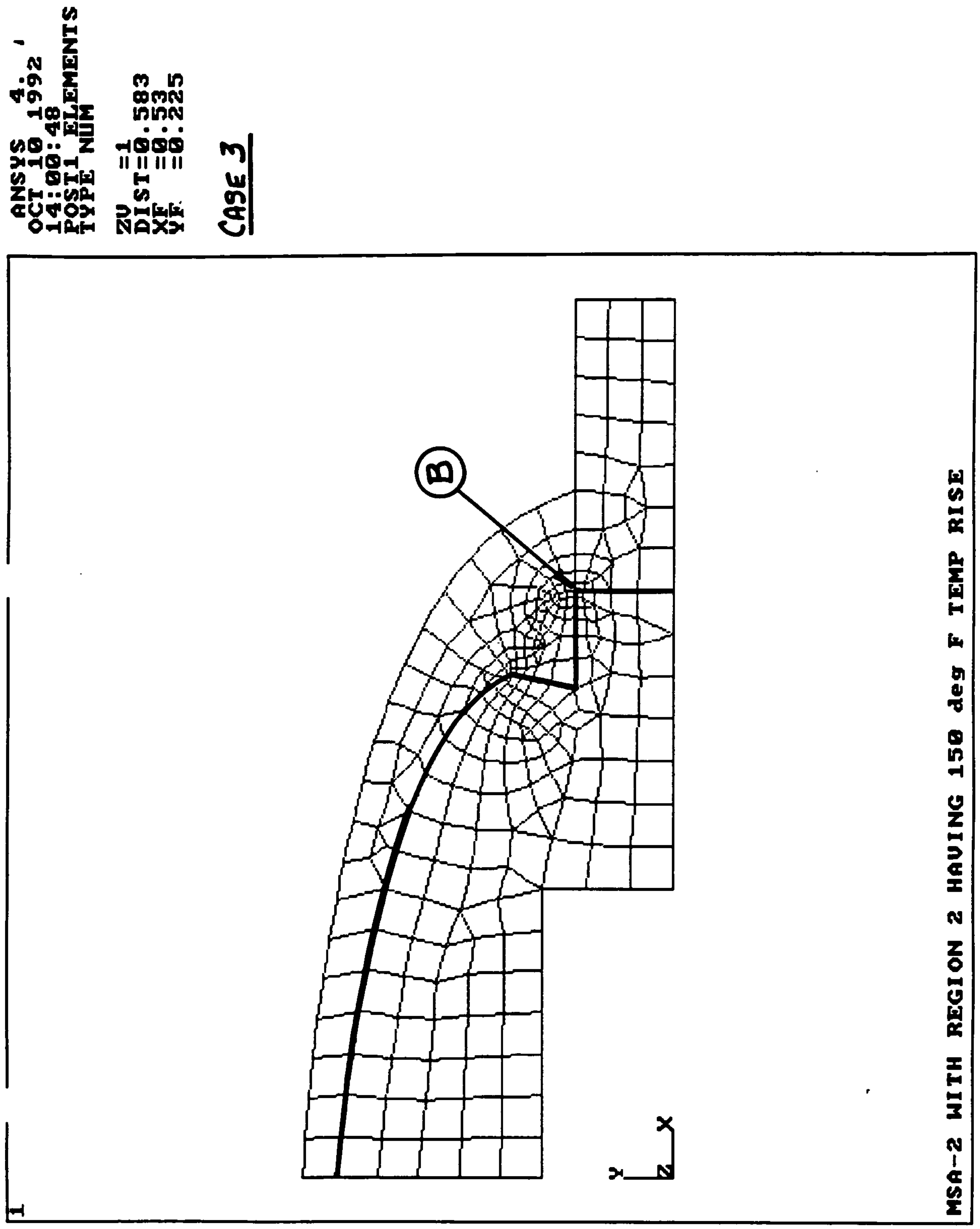
ANSYS 4.
OCT 10 1992
14:00:48
POST1 ELEMENTS
TYPE NUM
ZV =1
DIST=0.583
XF =0.53
YF =0.225
CASE 3
B
Y
X
Z
1
MSA-2 WITH REGION 2 HAVING 150 deg F TEMP RISE

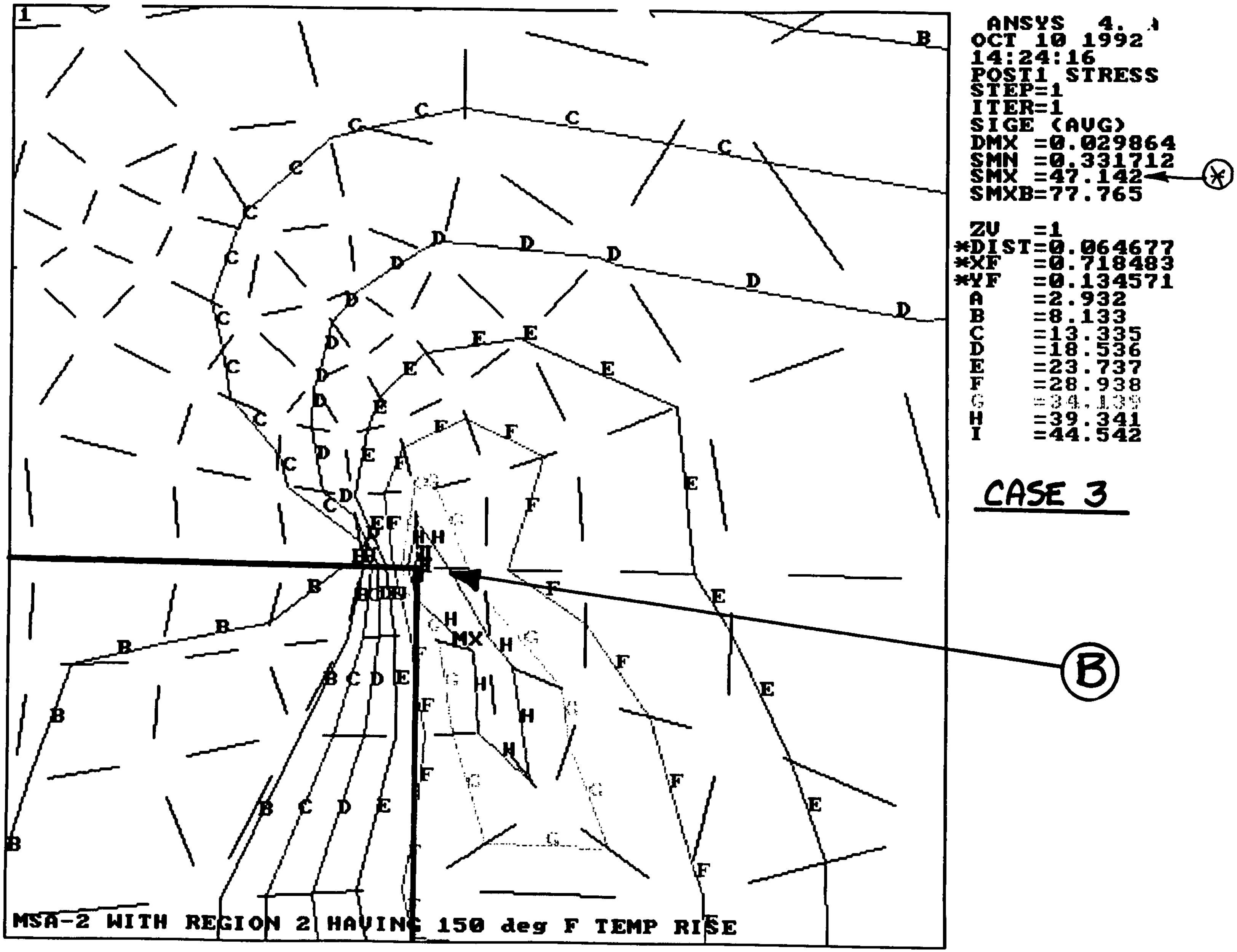
ANSYS 4.
OCT 10 1992
14:24:16
POST1 STRESS
STEP=1
ITER=1
SIGE (AVG)
DMX =0.029864
SMN =0.331712
SMX =47.142
SMXB=77.765
ZV =1
*DIST=0.064677
*XF =0.718483
*YF =0.134571
A =2.932
B =8.133
C =13.335
D =18.536
E =23.737
F =28.938
G =34.139
H =39.341
I =44.542
CASE 3
MSA-2 WITH REGION 2 HAVING 150 deg F TEMP RISE

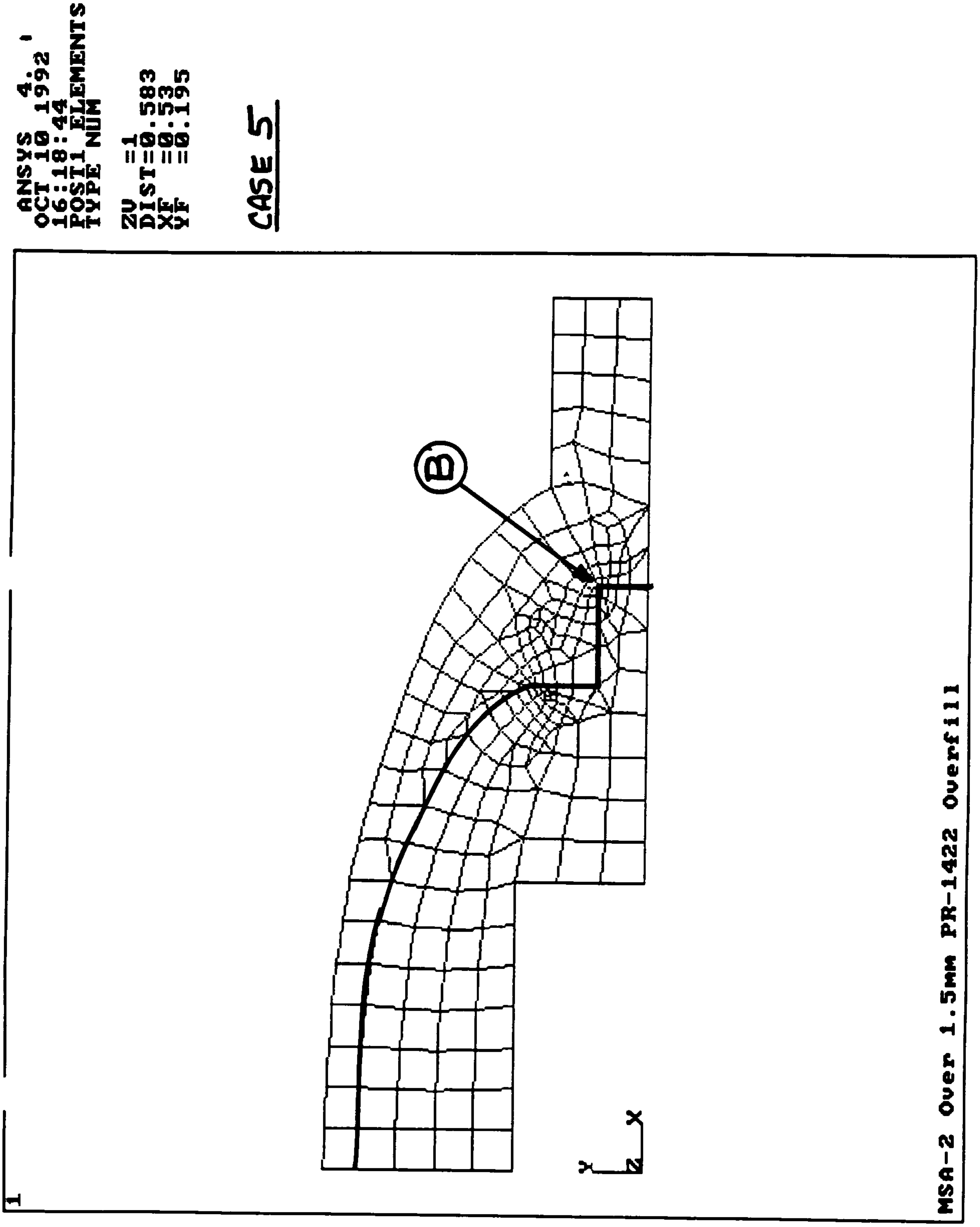
ANSYS 4.4
OCT 10 1992
16:18:44
POST1 ELEMENTS
TYPE NUM
ZV =1
DIST=0.583
XF =0.53
YF =0.195
CASE 5
B
MSA-2 Over 1.5mm PR-1422 Overfill

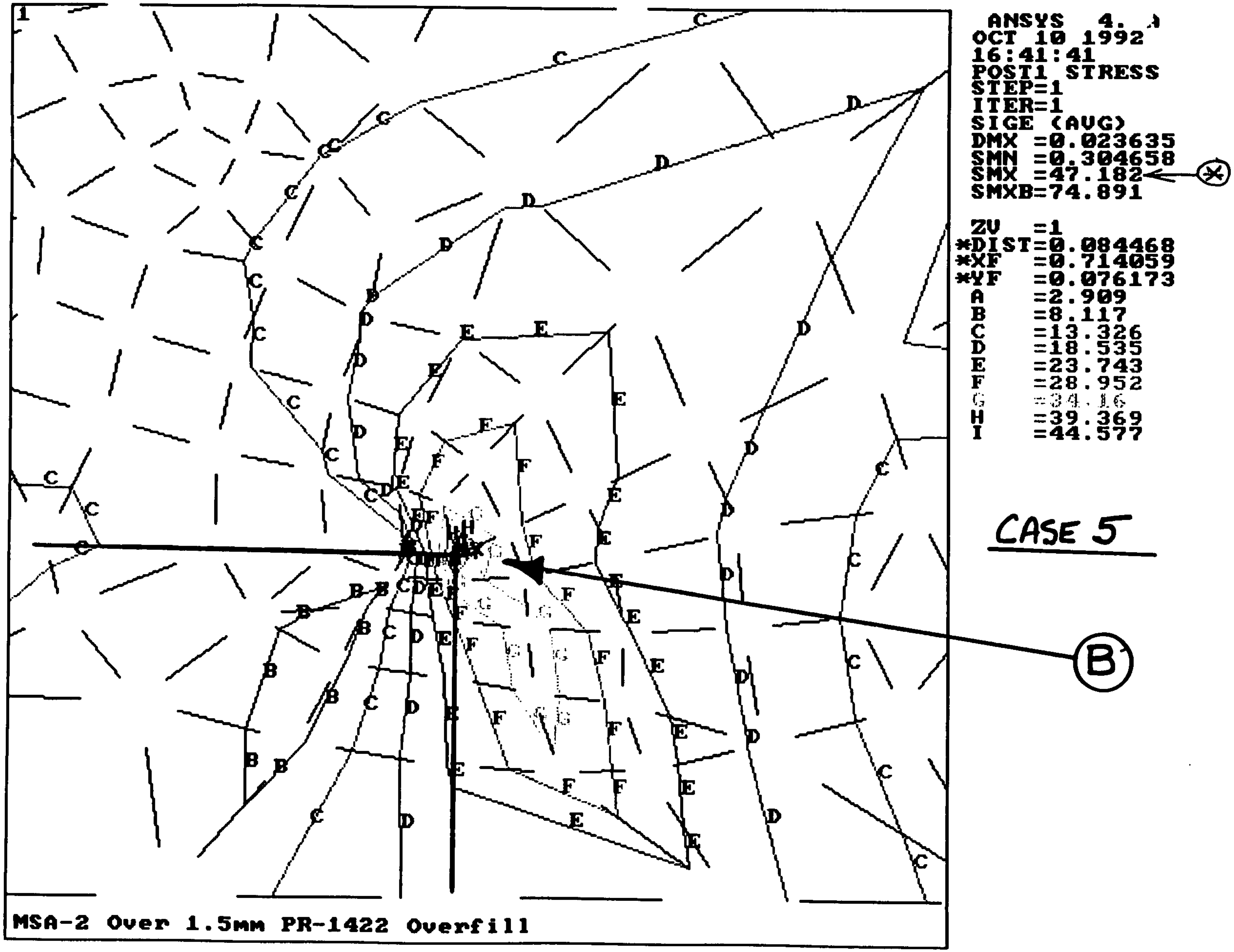
ANSYS 4. ?
OCT 10 1992
16:41:41
POST1 STRESS
STEP=1
ITER=1
SIGE (AVG)
DMX =0.023635
SMN =0.304658
SMX =47.182
SMXB=74.891
ZV =1
*DIST=0.084468
*XF =0.714059
*YF =0.076173
A =2.909
B =8.117
C =13.326
D =18.535
E =23.743
F =28.952
G =34.16
H =39.369
I =44.577
CASE 5
B
1
MSA-2 Over 1.5mm PR-1422 Overfill

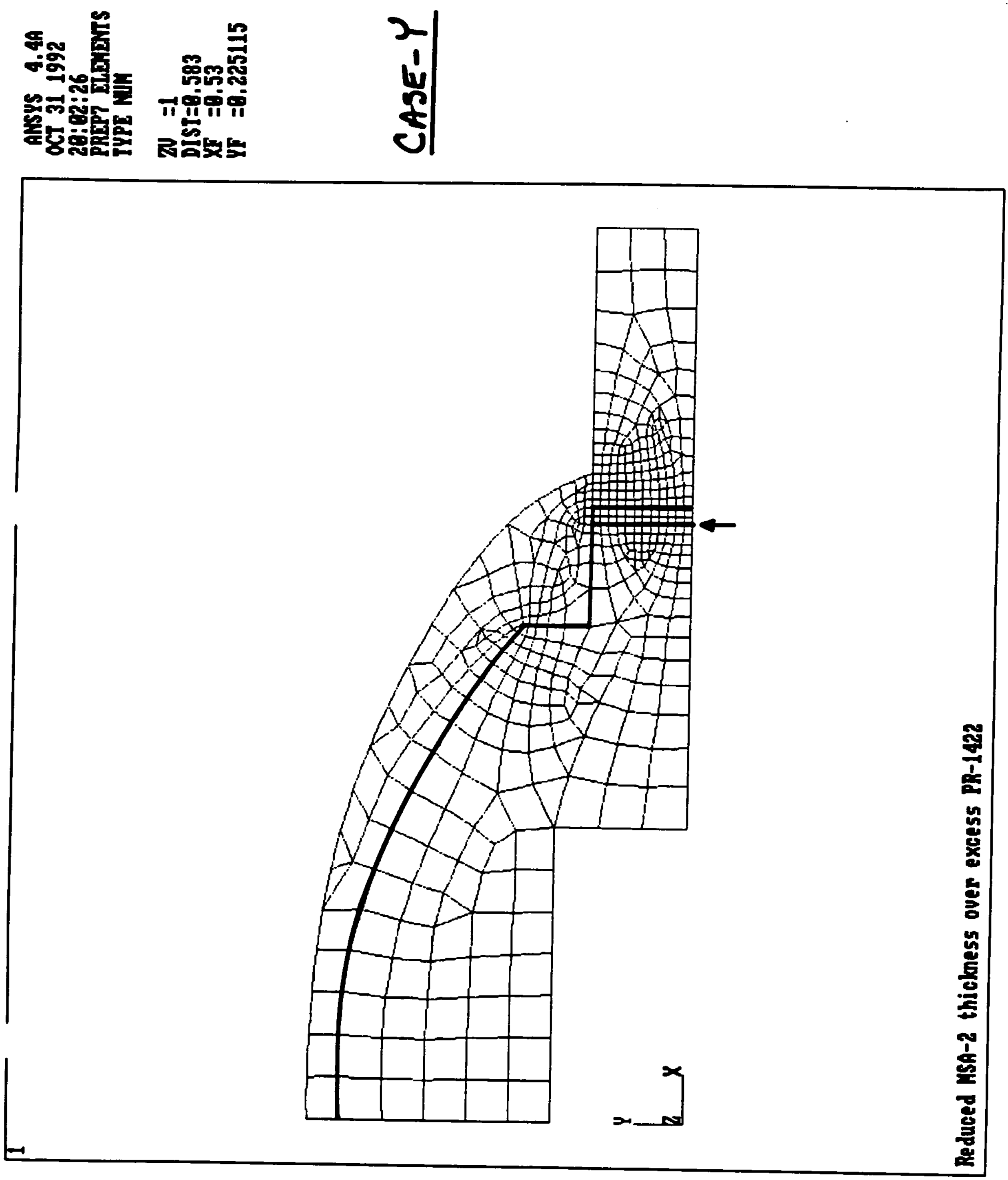
ANSYS 4.4A
OCT 31 1992
20:02:26
PREP7 ELEMENTS
TYPE NUM
ZV =1
DIST=0.583
XF =0.53
YF =0.225115
CASE-Y
Y
Z
X
Reduced MSA-2 thickness over excess PR-1422

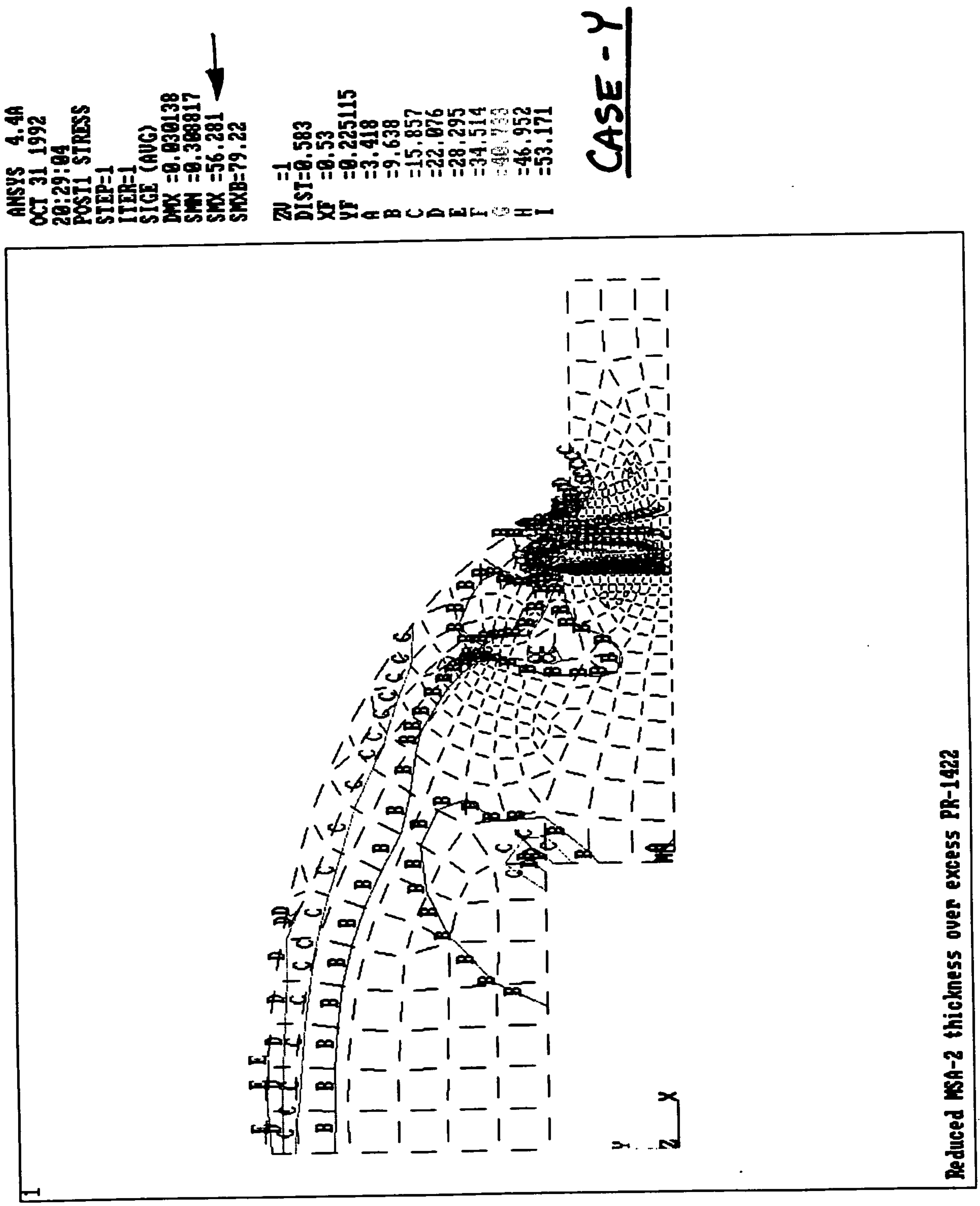

Reduced MSA-2 thickness over excess PR-1422

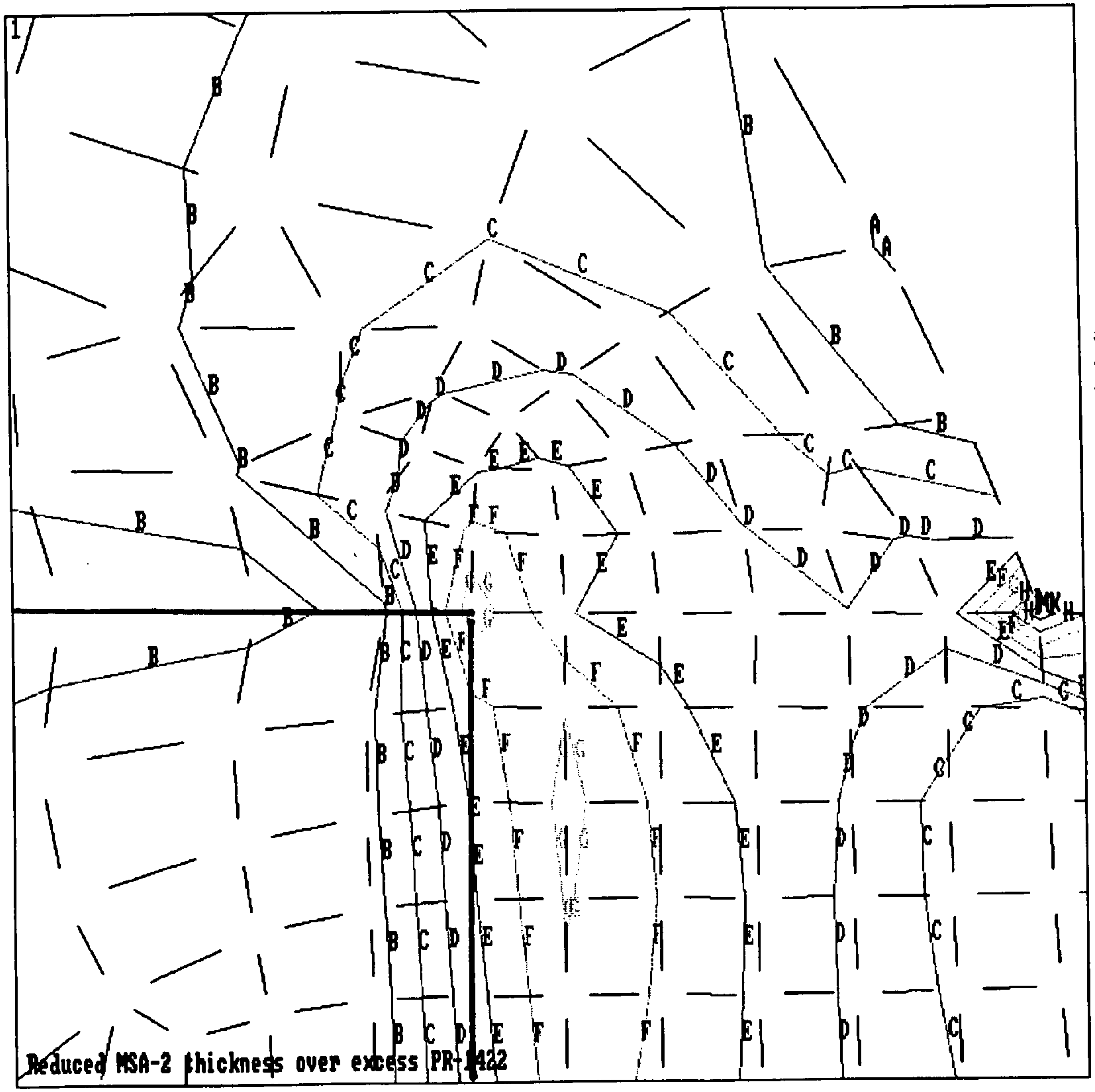

ANSYS 4.4A
OCT 31 1992
20:32:53
POST1 STRESS
STEP=1
ITER=1
SIGE (AVG)
DMX =0.030138
SMN =0.308817
SMX =56.281
SMXB=79.22

ZV =1
*DIST=0.056581
*XF =0.718483
*YF =0.128133
A =3.418
B =9.638
C =15.857
D =22.076
E =28.295
F =34.514
G =40.733
H =46.952
I =53.171

CASE-Y

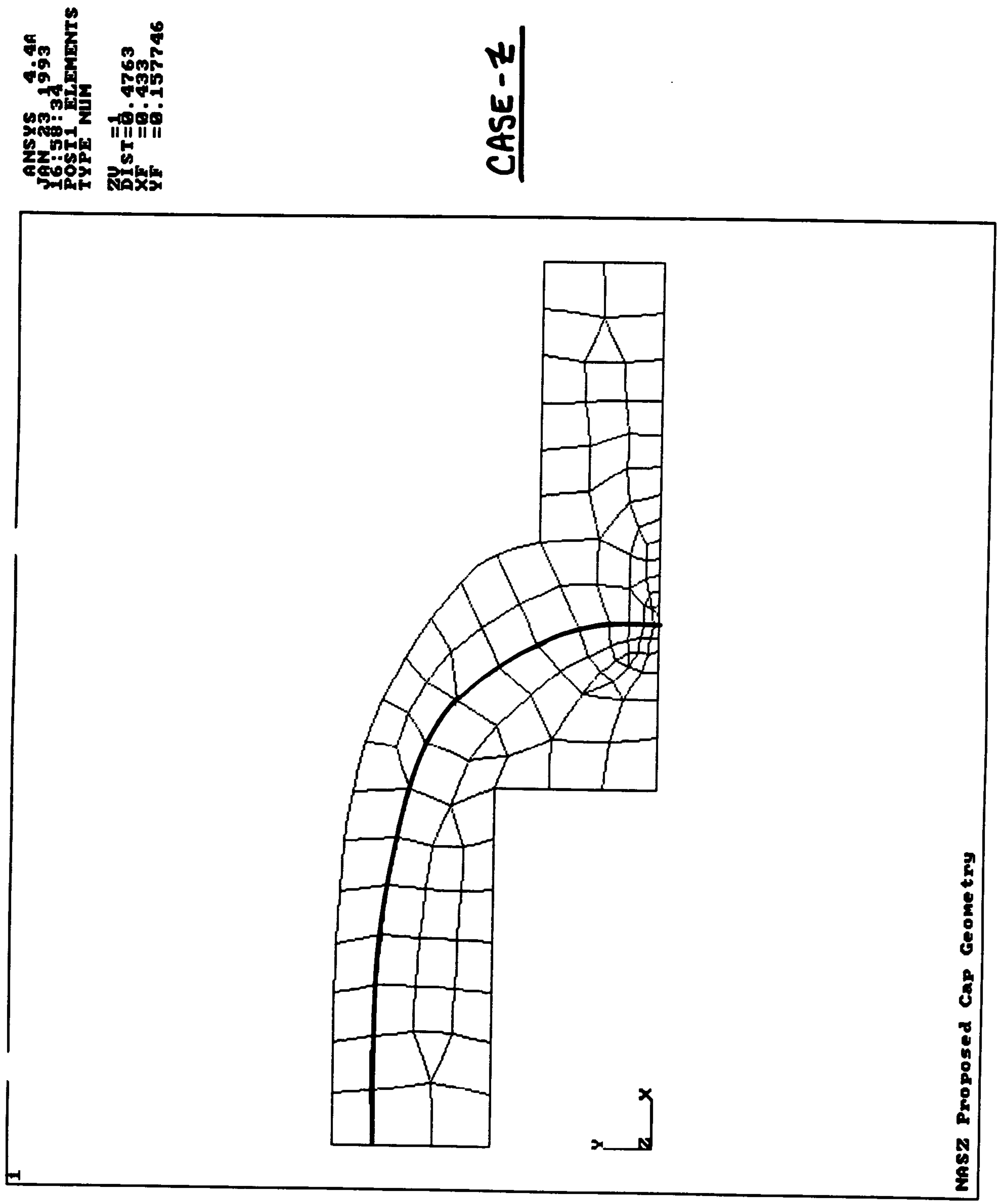
ANSYS 4.4A
JAN 23 1993
16:58:34
POST1 ELEMENTS
TYPE NUM
ZV =1
DIST=0.4763
XF =0.433
YF =0.157746
CASE-II
X
Y
Z
NAS2 Proposed Cap Geometry

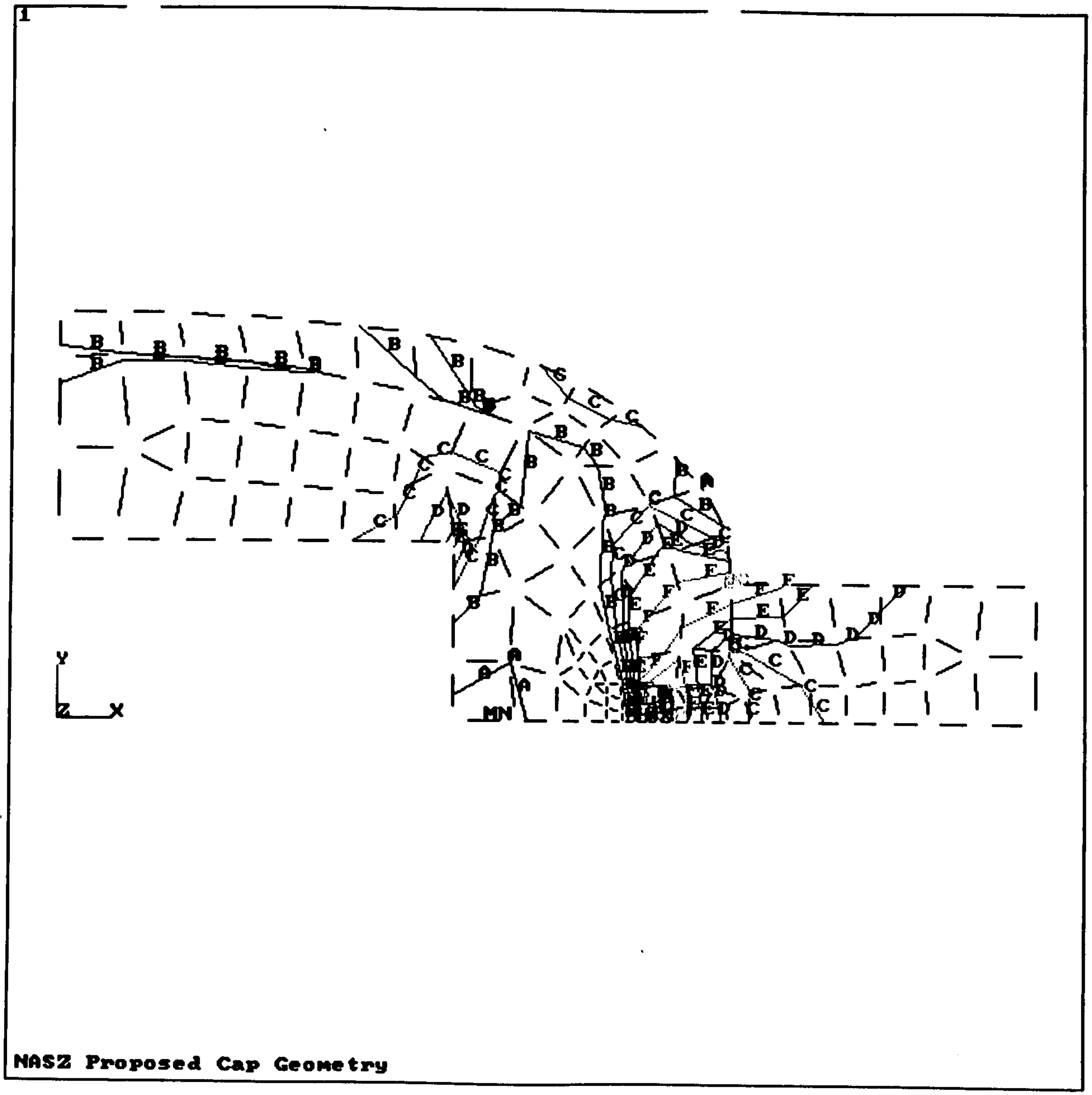

ANSYS 4.4A
JAN 23 1993
17:04:58
POST1 STRESS
STEP=1
ITER=1
SIGE (AVG)
DMX =0.012839
SMN =1.205
SMX =30.807
SMXB=46.742

ZV =1
DIST=0.4763
XF =0.433
YF =0.157746
A =2.85
B =6.139
C =9.428
D =12.717
E =16.006
F =19.295
G =22.584
H =25.873
I =29.162

CASE-4

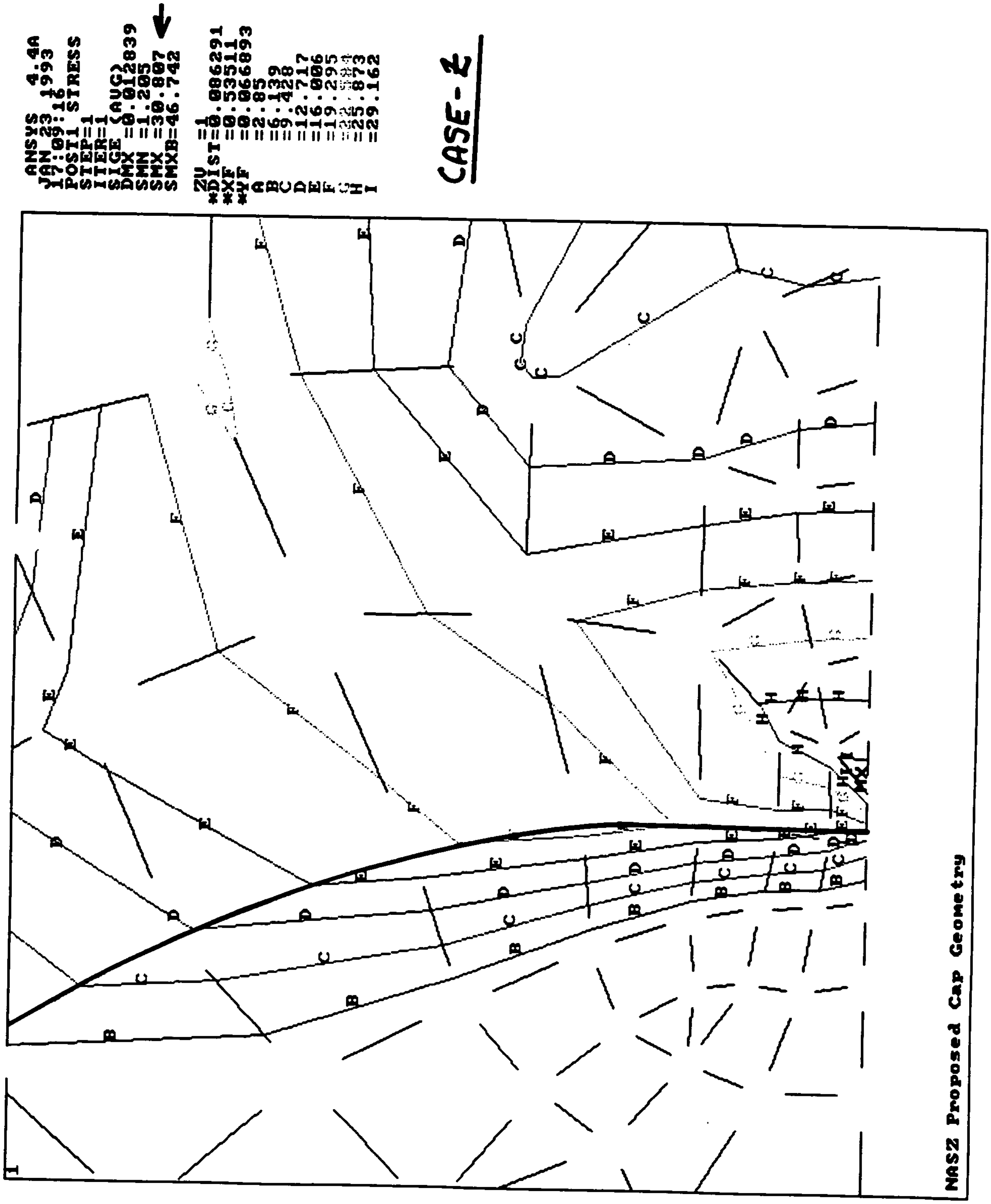

NAS2 Proposed Cap Geometry

REPORT DOCUMENTATION PAGE

Form Approved
OMB No. 0704-0188

1. AGENCY USE ONLY *(Leave blank)*

2. REPORT DATE
2/10/93

3. REPORT TYPE AND DATES COVERED
Final Report 17 August 92 to 15 Feb 93

4. TITLE AND SUBTITLE
SRB Frustrum "Smiley" Cracking Phenomenon Study

5. FUNDING NUMBERS
H11992

6. AUTHOR(S)
T. A. Cruse

7. PERFORMING ORGANIZATION NAME(S) AND ADDRESS(ES)
Thomas A. Cruse, Ph.D.
401 Bowling Avenue #6
Nashville, TN 37205

8. PERFORMING ORGANIZATION REPORT NUMBER
TAC-93-001

9. SPONSORING/MONITORING AGENCY NAME(S) AND ADDRESS(ES)
National Aeronautics and Space Administration
Marshall Space Flight Center
Huntsville, AL

10. SPONSORING/MONITORING AGENCY REPORT NUMBER

11. SUPPLEMENTARY NOTES

12a. DISTRIBUTION/AVAILABILITY STATEMENT
Unlimited Distribution

12b. DISTRIBUTION CODE

13. ABSTRACT *(Maximum 200 words)*

The thermal protection system installed on the SRB frustrums incurs the formation of debonds between the MSA-2 TPS material and the substrate. The debonds can lead to surface penetrating cracks, called "smileys" near sealed fasteners and other surface discontinuities. The study concluded that the "smileys" were caused as the result of stress risers caused by excess fastener sealant (PR-1422) and weakly bonded surfaces. Once the debond occurs, "smileys" form when the debond area is sufficiently large. The loading for the debond and "smiley" formation is seen to be depressurization at the vacuum conditions near the end of powered boost. The porous nature of the MSA-2 material covered by a vapor barrier paint provides internal pressure loading of the MSA-2 material. Recommendations for eliminating the problem include elimination of excess PR-1422 sealant and improved attention to bonding surface preparation.

14. SUBJECT TERMS
cracks,thermal protection,debonds,sealant

15. NUMBER OF PAGES
31

16. PRICE CODE

17. SECURITY CLASSIFICATION OF REPORT	18. SECURITY CLASSIFICATION OF THIS PAGE	19. SECURITY CLASSIFICATION OF ABSTRACT	20. LIMITATION OF ABSTRACT
Unclassified	Unclassified	Unclassified	UL